Master Thesis

Thermal Performance of Air Flow Windows

Lau Markussen Raffnsøe

supervisors:
Hans Janssen
Jianhua Fan

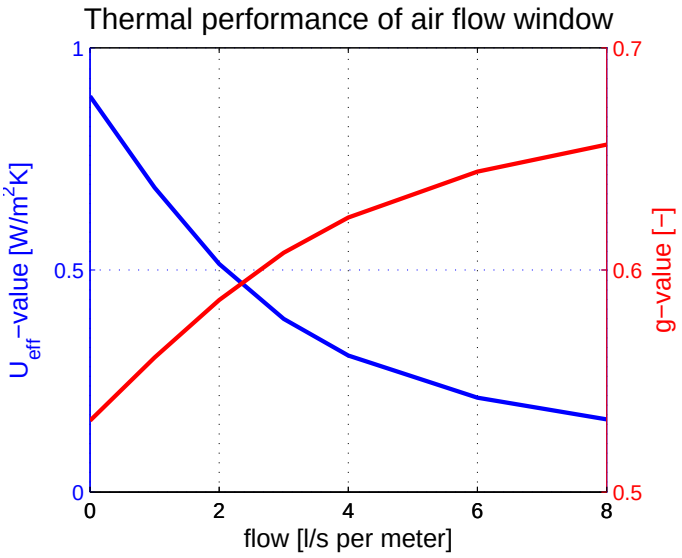

BYG•DTU
Department of Civil Engineering - July 2007

The present project is a master thesis project from the Technical University of Denmark and has been carried out from February 2007 to June 2007 at the Department of Civil Engineering BYG•DTU.

Typeset with Computer Modern
Layout by the author with the help of LaTeX
Figures made with WinFig
Graphs made with Matlab

Formal matters

The present report is a master thesis project from the Technical University of Denmark and has been carried out from February to June 2007 at the Department of Civil Engineering BYG•DTU.

Associate professor Hans Janssen and Jianhua Fan have been supervisors on this project.

The project is written by Lau Markussen Raffnsøe student at BYG•DTU. The project is prescribed to 35 ECTS points.

The project is handed in July 2nd and orally defended August 14th.

Lau Markussen Raffnsøe s021796

Abstract

Windows and ventilation are normally separate systems. At the maximum are fresh air valves placed in the frames of the windows. But air flow windows integrate windows and ventilation system by drawing the fresh air through the cavity between the panes before it enters the room. This report investigates the thermal performance of such air flow windows.

Based on extensive CFD modelling it is shown that the method prescribed by the existing ISO standard is inadequate in predicting the convective heat fluxes in the ventilated cavity. The basis of the existing standard is a representation of the cavity air temperature by the volume average temperature. It is demonstrated that the convective heat fluxes can not adequately be calculated based on this temperature representation. Therefore a new method based on a transient control volume method, is proposed and shown to produce significantly better predictions. The transient method is though not valid for flow patterns highly dominated by natural buoyancy, where it tends to underestimate the performance of air flow windows.

The transient method is implemented in a program called WinVent, developed in connection with this project. WinVent is based on the ISO standard and can calculate the thermal performance of normal windows as well as air flow windows, based on either the original standard method or the proposed transient method for the ventilated cavity.

Using WinVent the thermal performances of air flow windows are evaluated and compared to normal windows. Applying a low-emissivity hard coating on the inside pane of the cavity greatly increases the performance of the air flow window. A well designed air flow window can, with moderate to high ventilation flows, outperform even the best triple glazed windows with respect to both heat loss and solar gain.

There is a large potential for lowering heating demands in buildings with exhaust ventilation by using air flow windows. In an example of a 60 m^2 apartment it is calculated that air flow windows can reduce the total heat loss from windows and ventilation by almost 30%.

Resumé

Vinduer og ventilation er normalt separate systemer. Dog ses det ofte at friskluftventiler er placeret i vindueskarmene. Ventilationsvinduer integrerer vinduer og ventilation ved at lede den kolde ude-luft gennem hulrummet mellem glasruderne på vej ind. Denne rapport undersøger de energimæssige egenskaber af sådanne ventilationsvinder.

Ved brug af CFD modellering vises, at den gældende ISO standard ikke tilfredsstillende kan bruges til at beregne konvektive varmestrømme i det ventilerede hul i et ventilationsvindue. Den gældende standard forudsætter, at lufttemperaturen kan repræsenteres ved volumengennemsnittet. Rapporten viser, at denne forudsætning er utilstrækkelig i forhold til at beregne konvektive varmestrømme. Derfor foreslås at benytte en tidsafhængig kontrol volumen metode i stedet for, og det demonstreres, at den giver markant bedre forudsigelser. Forudsætningerne bag den tidsafhængige metode er dog ikke gyldige for strømningsmønstre domineret af naturlig opdrift, hvor metoden har en tendens til at undervurdere vinduets energimæssige ydeevne.

Den tidsafhængige metode er implementeret i programmet WinVent, der er udviklet i forbindelse med projektet. WinVent er baseret på ISO standarden og kan beregne de energimæssige egenskaber for både almindelige vinduer og ventilationsvinduer. For ventilationsvinduer kan WinVent beregne efter både den gældende ISO standard og den foreslåede tidsafhængige metode.

Ved brug af WinVent evalueres de energimæssige egenskaber af ventilationsvinduer i forhold til almindelige vinduer. Ventilationsvinduets egenskaber kan væsentligt forbedres med en hård lav-emissivitets belægning i det ventilerede hulrum. Et godt designet ventilationsvindue med moderat til høj ventilations mængde overgår selv de bedste tre-lags energiruder, både med hensyn til varmetab og sol energi transmittans.

Brug af ventilationsvinduer har et stort potentiale for at sænke opvarmningsbehovet i bygninger med udsugningsventilation. Et eksempel med en 60 m^2 lejlighed viser at det samlede varmetab fra vinduer og ventilation kan reduceres med næsten 30%.

Contents

Nomenclature

Symbol	Definition	Units
English letter symbols		
a	variable	$-$
A	Area	m^2
c_p	specific heat capacity at constant pressure	$J/(kg\,K)$
d	depth of cavity	m
g	total solar energy transmittance	$-$
	or gravity constant	m^2/s
Gr	Grashof number – ratio of buoyancy to viscous forces	$-$
h	height	m
	heat transfer coefficient	$W/(m^2K)$
H	Height of window cavity	m
H_0	characteristic height – penetrations length of ventilation air	m
I^+	flux of solar irradiation between panes in direction from towards outside	W/m^2
I^-	flux of solar irradiation between panes in direction from towards inside	W/m^2
J	radiosity, flux of long wave radiation between panes	W/m^2
L	characteristic length	m
Nu	Nusselt number	$-$
q	specific energy flux	W/m^2
Q	energy flux	W

continues

Symbol	Definition	Units
Q_{adv}	advective energy flux, energy transported with the ventilation air	W
Q_{in}	energy flux form indoor environment to window	W
Q_{out}	energy flux form window to outdoor environment	W
Q_{vent}	ventilation heat loss, energy needed to heat ventilation air from outdoor to indoor temperature	W
R	thermal resistance	m^2K/W
Ra	Rayleigh number	$-$
Re	Reynolds number – ratio of inertia to viscous forces	$-$
S	absorbed solar radiation	W/m^2
T	Temperature	K
u	velocity component in specific direction	m/s
U_{eff}	effective U-value	W/m^2K
U_{vent}	ventilation U-value	W/m^2K
U_{tot}	total U-value, $U_{tot} = U_{eff} + U_{vent}$	W/m^2K
V	average velocity	m/s
y_p	distance from wall to first mesh point	m
y_p^+	dimensionless number that characterize the flow at the first mesh point	$-$
x, y, z	cartesian coordinate axes	$-$

Greek letter symbols

β	volumetric thermal expansion coefficient	$1/K$
ε	surface emissivity	$-$
λ	thermal conductivity	$W/(m \cdot K)$
μ	dynamic viscosity	$N \cdot s/m^2$
ν	kinematic viscosity	m^2/s
ρ	density or specular reflectance	kg/m^2 $-$
σ_s	Stefan-Boltzmann constant $5.67 \cdot 10^{-8}$	$W/(m^2K^4)$

continues

Symbol	Definition	Units
τ	transmittance	$-$
φ	volume flow	m^3/s

Subscripts

av	surface average
avg	volume average 6
b	backside of pane (facing inwards)
c	convection
cav	cavity
cv	convection for ventilated cavity
f	front side of pane (facing outwards) or forced convection
g	glass
i	number of pane
in n	inside environment natural convection or direction towards inside environment
out	outside environment or direction towards outside environment
rad	radiation
tra	transient method
ISO	ISO standard method

Chapter 1

Introduction

1.1 Background

Starting with the Danish energy crisis in the 1970'ties there has been an increasing focus on lowering energy consumption in buildings. In recent years it is not so much the actual heating cost, but environmental issues, that have driven the progress towards low energy and heating demands in buildings. In the first many years focus was on transmission heat loss through the building envelope. This is exemplified by the Danish building regulation code of 1977 [1], that introduces almost a doubling of minimum insulation of building envelope and a maximum allowable window area at 15% of the floor area.

Since then legislative tightenings of the energy demands in buildings have regularly been introduced. And with advances in window technology and subsequently significant improvement of windows thermal performance the tight restrictions on window area have been omitted. But windows and doors still count for a significant portion of the total heat loss.

As buildings have become increasingly better insulated, ventilation heat loss has an increasing influence. In well insulated houses the ventilation heat loss can easily be greater than the transmission heat loss through the building envelope. This has of course brought focus on air tightness and controlled ventilation flow. Older buildings are almost always naturally ventilated through leaks in the building envelope. But with improved air tightness of the building envelope the natural ventilation is often too small to prevent damp buildings and associated problems like mold. The problem is intensified by many occupants' reluctance, because of the heating cost, to open windows for venting.

To ensure minimum ventilation rates it is demanded that at least a mechanical exhaust ventilation system is installed. The fresh air is then supplied

through fresh air valves, often placed in the window frames. In the Danish building regulation code [2] the minimum ventilation rate for the average apartment is 0.5 air change per hour $[0.5h^{-1}]$ or 35 l/s, whichever is highest[1].

Balanced ventilation systems with heat recovery can significantly reduce the ventilation loss, but have only recently begun to find favour in the building industry and almost exclusively in commercial buildings and single family houses. Commercial buildings often have high ventilation rates and therefore heat recovery has a much greater impact. For single family houses heat recovery ventilation systems have primarily been installed by environment and energy conscious building owners. But recent legislative tightening of energy demands of buildings has made it difficult to avoid heat recovery ventilation systems in new commercial buildings and single family houses.

But for apartment blocks the incentive to install heat recovery ventilation is in many cases still absent. The new building regulation code of 2006 [2] introduces a total energy frame that the buildings must maintain. But for apartment blocks a supplement to the energy frame is given if only exhaust ventilation is installed. The motivation behind the supplement is that small apartments, especially dormitories or dwellings for senior citizens, have a very high ventilation rate. In order not to punish small apartments unjustly they are given a supplement to the energy frame for exhaust ventilation exceeding 0.3 l/s per m^2 floor area - roughly equivalent to an airchange of 0.5 times per hour. For example, a 40 m^2 apartment has a minimum ventilation rate of 1.2 airchange per hour. Therefore many new apartment blocks are still build with exhaust ventilation systems only.

In any case does legislative tightening of the energy demands only affect new and future buildings. But most of the energy consumption is in old buildings. In order to reduce energy demands in the building sector significantly the older building stock needs to be modernized. But for the majority of the existent multi storey buildings it is a costly and difficult affair to install balanced ventilation.

Balanced ventilation with heat recovery is not the only solution to lower ventilation heat loss. Another proposed solution to lower heating demands in exhaust ventilated buildings is the air flow window. The concept is also known as supply air window and ventilation window.

[1]For multistory buildings the minimum exhaust ventilation is defined as 15 l/s for bathroom/toilet and 20 l/s for kitchen, or an air change of 0.5^{-h}.

1.1.1 Air Flow Window

”Air flow window” is often used to describe a multiple pane window, where one or more cavities are ventilated. In cold conditions the intake of fresh air can be led through the ventilated cavity and thereby preheat the fresh air and hopefully reduce the overall heat loss. In warm sunny conditions the ventilation air in the cavity can be returned to the outside and thereby reduce the heat load from absorbed radiation in the window construction. Air flow window is the main principle for multiple skin facades systems.

Research has indicated that the principle of air flow windows can be used to improve the energy balance for windows in both heating and cooling conditions. It is reported that the effective U-value can be reduced with as much as 30-40% [3–8].

The thermal performance of air flow windows appears to change greatly with the operating conditions, especially ventilation flow rate. The thermal performance can in fact not be assessed without including the ventilation system, because the ventilation air led through the window, even though it becomes preheated, still needs to be heated to indoor room temperature.

If the choice stands between normal windows combined with heat recovery ventilation system or air flow windows combined with exhaust ventilation system, then air flow windows are not necessarily the best choice. But if the other option is normal windows combined with exhaust ventilation or maybe a natural ventilation system, then air flow windows appear to have significant advantages. The overall heat loss can be reduced and, because of the preheating of the ventilation air, the risk of draught is also reduced.

There are already air flow window products on the market [9, 10], see figures 1.1 and 1.2 on the following page. But the development and market impact of these window types is, among other things, hindered by the lack of reliable and simple methods for prediction of the energy balance for the window. The thermal performance of air flow windows can not easily be described by a simple U-value and g-value. It is therefore not easy, if even possible, for potential consumers to compare the energy impact of different air flow window types, nor compare air flow windows with normal windows. This makes the current use of air flow windows a matter of belief more than a matter of rational consideration.

The international standard *ISO 15099, Thermal Performance of Windows, Doors and Shading Devices - Detailed Calculations* [11], hereafter just referred to as the ISO standard, does prescribe a method for calculating U-value and ventilation heat gain for windows with ventilated cavity. This method is also implemented in the WIS[2] program. But the use of the standard is not

[2]The WIS program is made freely available by the Windat organization `www.windat.`

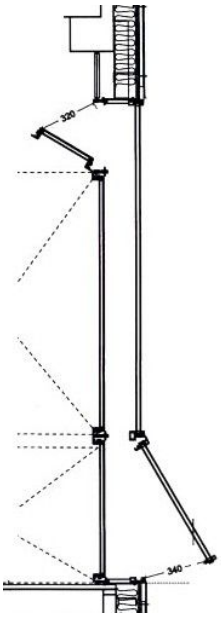

FIGURE 1.1: *3G window by Hansen Group [9]*

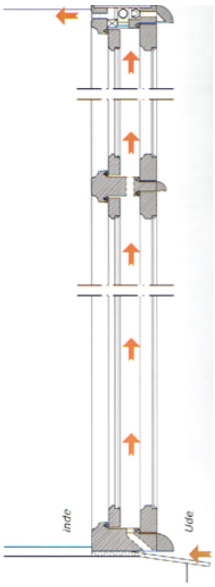

FIGURE 1.2: *Ventilation window by PCvinduer [10]*

wide spread, and of all the literature studied in connection with this project only one, [3], relates to the ISO standard.

This can probably be explained by the fact that the ISO standard method for air flow windows is not well documented. The differences between normal windows and air flow windows are the convective and advective heat fluxes in the ventilated cavity. As this project will show, the ISO standard method has some obvious problems in predicting these heat flows. The ISO standard actually states that the chapter concerning ventilated cavity, *must be considered as provisional and is provided for information purposes only.*

1.2 Aim and Methodology

The fundamental motivation behind this project is a desire to evaluate the thermal performance of air flow windows and thereby illustrate the potential energy savings that a rational use of air flow windows present. But there is apparently a lack of adequate methods for calculating the convective heat fluxes in ventilated cavity in air flow windows. None of the literature studied in connection with this project have suggested a method other than CFD simulations. Nor can the ISO standard method adequately describe the convective

org

heat flows. The calculation method presented in the ISO standard, will in this project in fact be shown to have fundamental shortcomings.

Conduction, radiation and convection in enclosed cavity are all very well understood and described. But, as we will se, convection in a *ventilated* cavity is quite difficult and not very well understood nor described.

1.2.1 Aim

It is the therefore the aim of this project to propose a satisfying method for calculating the thermal characteristics of air flow windows in order to evaluate the thermal performance. The efficiency of the air flow windows, compared to normal windows, is mainly dependent on the thermal characteristics of the ventilated cavity. The main issue is the convective heat fluxes in the ventilated cavity. Establishing a more precise and well founded method for prediction of convective heat fluxes in ventilated cavity will lead to a more reliable method for predicting the thermal performance of air flow windows.

1.2.2 Methodology

The critical heat fluxes are the convective heat transfers between the surfaces of the panes and the air in the cavity. Convective heat fluxes depend on temperature differences and flow pattern of the fluid. The air flow pattern and as such the convective heat fluxes may change greatly with the specific geometry of the window and the external conditions like solar irradiation and ventilation flow rate. The short time frame and the need to analyze many different configurations make CFD modeling the tool of choice for this part of the project. CFD simulations can, if done correctly, give very precise and detailed information on the physical properties of the flow, like heat fluxes and temperatures. Each simulation may take hours, but change of parameters is fast and multiple simulations can be conducted simultaneously, depending on the number of computers available. By using CFD modeling as the main tool for investigation, it is possible to conduct a much larger parameter study, than would be possible with experimental tests.

By analyzing the relationship between the specific geometry, external conditions, surface temperatures and convective heat fluxes, it should be possible to either prove the ISO standard method adequate, despite its shortcomings, or suggest another method. The possible methods investigated are based on:

- changing of the ISO standard
- using a transient analysis of the temperature development up trough the cavity

The Transient method produces remarkably good results based on very simple assumptions, while the ISO standard method is shown to have a fundamental flaw in its representation of the cavity air temperature.

The transient calculation method for the ventilated cavity is implemented in at calculation of the thermal performance of whole air flow windows. In connection with this project a program called WinVent has been developed based on the ISO standard, that incorporates both the original ISO standard method for the ventilated cavity and the transient method.

The scope of this project is limited to the glass area of the window, and does only very briefly deal with heat flows in the frame area. When there in this document is referred to window, it is actually only the vision area that is meant. The geometry of the necessary valves in the frame is of cause important for the air flow pattern in the cavity and will therefore, in some degree, be taken into account. WinVent only calculates the vision area though and does not include frame area nor shading devices. How the valves influence the heat loss through the frame is outside the scope of this report.

WinVent is used, with the transient method for the ventilated cavity, to evaluate the thermal performance of air flow windows under specified conditions (ventilation flow). The ventilation flow depends of course on the flow resistance and pressure difference across the window. But specifically how the pressure difference is achieved is the subject of a whole building analysis, and is therefore outside the scope of this project. But it is the aim that the method developed by this project can be implemented in dynamic building performance assessment programs like the research oriented programs Building Physics Toolbox [12] and BuildingCalc [13] or commercial programs like BSim [14] and IESVE [15].

1.3 Overview of Chapters

2. Detailed calculation of Windows Energy Balance

First in this chapter the thermal performance characteristics of air flow windows are defined. Then the ISO standard method for calculating the thermal performance for the vision area of normal windows and air flow windows is presented. Special emphasis is placed on the convective heat fluxes in a ventilated cavity.

3. Description and Validation of CFD Models

The CFD model used for the parameter study of the convective heat fluxes in a ventilated cavity is described in detail. The description includes geometry, boundary conditions, mesh generation, near wall treatment, turbulence

model and radiation model. The model is validated by grid dependency analysis, and by verification of the turbulence model by comparison to reference data of natural convection in closed cavity, which is a well known and extensively researched case. The reference data is the ISO standard method for unventilated cavities.

4. CFD Simulation Results
The results of the parameter study of the ventilated cavity are presented and compared to ISO standard calculations.

5. Analysis of CFD Simulation Results
Two different approaches to improve the calculation method for the ventilated cavity is analyzed:

- Improvement of the multi-node resistance model that ISO standard method is based on.
- Transient heat flux and temperature development with the time dependency linked to the height of the cavity.

The transient model is found to produce the overall best results.

The last section presents how the transient model is implemented in the WinVent calculation of the thermal performance for the whole window. The calculation method for the whole window is based on the ISO standard.

6. Thermal Performance of Air Flow Windows
With the use of WinVent, the thermal performance characteristics of two different designs of airflow windows are calculated for a range of ventilation flows. The thermal performances are compared to normal windows in situations with exhaust ventilation. The windows energy balances for the heating season are evaluated for na example of a 60 m^2 apartment.

The influence of the cavity design on the thermal performance characteristics is discussed. Including a more general discussion of some of implications for the design of air flow windows not covered in the main analysis.

The air flow windows performance in summer conditions are discussed briefly.

7.3. Further Work While contributing with a important basis for advancing the knowledge and use of air flow windows, this project only lays out at promising path to follow. Many issues still needs to be understood better if the potential of air flow windows are to be utilized. No to mention the task

of optimizing the design – including design of frame and valves. This chapter concerns ideas to projects which could be made in continuation of the present project.

7. Discussion and Conclusion

The project is summarized and the main findings presented in the conclusion.

Chapter 2

Detailed Calculation of Windows Energy Balance

Air flow windows have a more complicated energy balance and thermal performance characteristics than normal windows. This chapter therefore first gives a detailed description and definition of the thermal performance characteristics.

The governing equations for the energy balance of windows implemented in the WinVent program are described in the second part of the chapter. The WinVent program is based on the ISO standard. The ISO standard method can be considered as the existing benchmark for prediction of the convective heat fluxes in ventilated cavities. Any alternative method is only interesting if it significantly improves the prediction of thermal performance. It is therefore appropriate to present a detailed description of the governing equations that constitute the ISO standard method.

2.1 Thermal Characteristics of Air Flow Windows

The thermal characteristics of normal windows are split into a heat loss factor, U-value, and a solar heat gain factor, g-value. The U-value is the heat transfer coefficient and is a measure for how much heat is lost for a given temperature difference between in- and outside. Sometimes, especially in the US, it is called *dark U-value*, because it is calculated for ”dark” conditions without solar radiation. The g-value is the total solar energy transmittance and is a measure for how much of the incident solar radiation on the window is utilized as heat gain indoors. The g-value includes both the solar radiation directly transmitted through the window and the effects of absorbed solar radiation heating the panes.

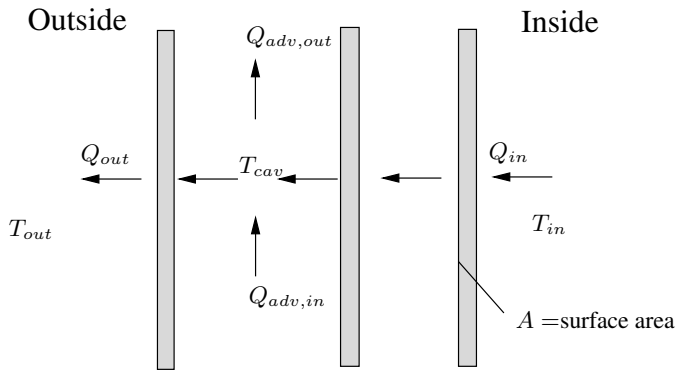

FIGURE 2.1: *General heat flows for ventilated window. The arrows indicate the positive direction, not necessarily the actual direction.*

For a window without ventilated cavities, the U-value is calculated as the reciprocal of the total thermal resistance.

$$U = \frac{1}{R} \qquad [W/m^2K] \tag{2.1}$$

Where:

$$R = \frac{1}{h_{out}} + \sum R_i + \sum R_{g,i} + \frac{1}{h_{in}} \tag{2.2}$$

and R_i is the thermal resistance of the i'th cavity and $R_{g,i}$ is the thermal resistance of the i'th glazing.

But when one or more cavities are ventilated with supply air, a portion of the heat flow through the inner surface is regained as preheated fresh air. The heat flow is therefore no longer constant through the different layers and the heat flows through the inner and outer panes are not only dependent on the combined thermal resistance.

U$_{eff}$ Under the assumption, that the building has exhaust ventilation and fresh air in any case needs to be supplied, an effective U_{eff}-value is defined that enables easy comparison between the heat balance for a normal window with fresh air valves and the ventilation window. By placing the boundary between indoor and outdoor on the outside of the window, the only difference between a normal window and the ventilated window is the heat loss through the outer pane. The ventilation heat loss is the same for the two types, because the boundary is placed before any preheating takes place. The U_{eff}-value is therefore defined as heat loss through the outer pane, q_{out} normalized by the temperature

difference between inside and outside, equation (2.3). The parameter U_{eff} is the main parameter that describes the effect of the air flow window, and is also used by [7] and [8].

U$_{vent}$ The U_{vent} value is defined as the the ventilation heat loss coefficient, equation (2.4). The ventilation heat loss is the energy needed to heat the ventilation air from outdoor temperature to room temperature, per m^2 window area, equation (2.22). Not to be confused with $Q_{adv,in}$ or $Q_{adv,out}$, that are the advective energies respectively entering and leaving the ventilated cavity.

U$_{tot}$ The U_{tot} value is defined as the coefficient for the total heat loss due to the window, including both the ventilation loss and the transmission heat loss through the window, equation (2.5). The U_{tot} is the sum of U_{vent} and U_{eff}.

g-value The g-value is a measure for how much of the solar radiation is utilized as heat gain. In keeping with the recommendations by [8]. This includes both direct and indirect radiation, radiation absorbed in the panes and convected/radiated into indoor environment and additional preheating of the ventilation air, equation (2.6).

$$U_{eff} = \frac{Q_{out}}{A(T_{in} - T_{out})} \qquad [W/m^2K] \qquad (2.3)$$

$$U_{vent} = \frac{Q_{vent}}{A(T_{in} - T_{out})} \qquad [W/m^2K] \qquad (2.4)$$

$$U_{tot} = \frac{Q_{out} + Q_{vent}}{A(T_{in} - T_{out})} = U_{eff} + U_{vent} \qquad [W/m^2K] \qquad (2.5)$$

$$g = \frac{(q_{vent} + q_{in}) - (q_{vent} + q_{in})(I_s = 0)}{I_s} \qquad [-] \qquad (2.6)$$

$$(2.7)$$

Where:

Q_{out} is the heat flow from the window to outside environment $[W/m^2]$.

Q_{vent} is the ventilation heat loss through the ventilation window, defined as energy needed to heat the ventilation air to room temperature, equation (2.22) normalized per square meter window $[W/m^2]$.

$(Q_{vent} + Q_{out})(I_s = 0)$ is the combined heat loss from the window, including ventilation, for the specified conditions, but without incident solar radiation $[W/m^2]$.

A is the surface area of the window (vision area), $[m^2]$.

By knowing both the U-value(s) and g-value it is possible to calculate the thermal performance of the window under any conditions of temperatures and solar radiation.

This is of course only true under the assumption that the U-value and g-value are constant. Because the material constants of the cavity gases are temperature dependent, the U-value is in fact not constant but dependent on the in- and outside temperatures. To simplify heat loss calculations the U- and g-values are calculated in accordance with the ISO standard for standard winter conditions and considered to be constant in the relevant temperature range. The standard conditions are presented in table 2.1. Because this project focuses on the heat loss, only the winter standard conditions will be applied.

condition	notation	winter	summer	designation
Indoor air temperature	T_{in}	20	25	°C
Outdoor air temperature	T_{out}	0	30	°C
Indoor convective heat transfer	$h_{c,in}$	3.6	2.5	W/m^2K
Outdoor convective heat transfer	$h_{c,out}$	20	8	W/m^2K
Indoor radiation temperature	$T_{r,in}$	T_{in}	T_{in}	°C
Outdoor radiation temperature	$T_{r,out}$	T_{out}	T_{out}	°C
Incident solar radiation	I_s	300	500	W/m^2

TABLE 2.1: *Reference boundary conditions*

2.2 ISO Standard Method Implemented in WinVent

This is a detailed description of the equations that constitute the energy balance for a ventilation window. It is a one-dimensional calculation and temperature nodes are placed in the centre and on the surfaces of each glazing and in the centre of the ventilated cavity. Even though it is a one-dimensional calculation is the *vertical* temperature variation of the air in the ventilated cavity considered. The notation is attempted to be in accordance with ISO standard [11], to ensure an easy comparison.

The heat flow in a window can be broken down into different types of heat flow:

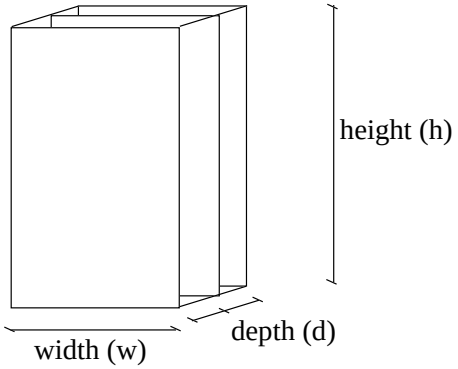

FIGURE 2.2: *Overall dimensions for window*

- convection in the gas between the glass panes and to the surrounding environments
- conduction in the glass panes
- radiation across the cavities and to the surroundings
- advective heat flows, due to temperature difference between ventilation air entering and leaving the cavity.

These types of heat flows will be described in detail in the following.

2.2.1 Convective heat Transfer

When the cavity is ventilated not only the convective heat flux between the surfaces has to be taken into account, but also the advective heat flux due to temperature differences between the air entering or leaving the domain. The notation can be seen in figure 2.3 on the following page. Q_{cv} is the heat flux from the glazing surface to the air in the cavity – temperature node T_{cav}. The subscriptions (f) and (b) are used to indicate the front or the back side of the corresponding pane(i) and not the cavity.

$$Q_{cv,f,2} = h_{cv,1} A (T_{f,1} - T_{cav}) \qquad [W] \qquad (2.8)$$

$$Q_{cv,b,1} = h_{cv,1} A (T_{cav} - T_{b,2}) \qquad [W] \qquad (2.9)$$

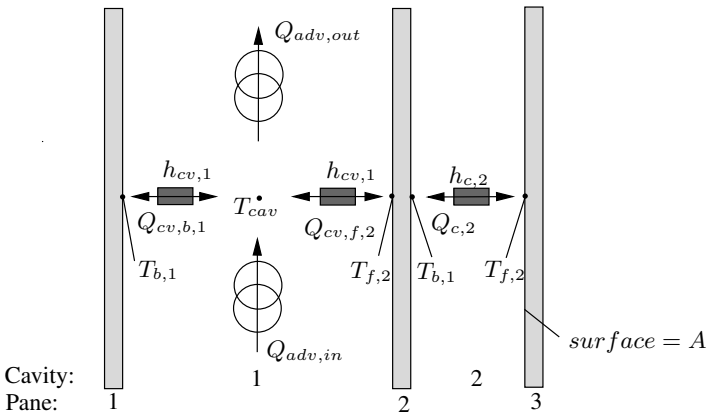

FIGURE 2.3: *Heat balance for the ventilated cavity*

In case of no ventilation of the cavity the convective heat transfer can be reduced to surface to surface convection. In ISO standard the surface to surface convective heat transfer is the main equation, and surface to cavity is an extension/complication only used for the ventilated cavity case.

$$Q_{c,2} = h_{c,2}A(T_{f,3} - T_{b,2}) \tag{2.10}$$

Where:

$Q_{cv,b,1}$ is the convective heat transfer from the ventilated cavity to pane 1, $[W/]$.

$Q_{cv,f,2}$ is the convective heat transfer from pane 2 to the ventilated cavity, $[W/]$.

$h_{cv,1}$ is the surface to air convective heat transfer coefficient for the ventilated cavity, given by equation (2.13), $[W/m^2K]$

$h_{c,2}$ is the surface to surface convective heat transfer coefficient given by equation (2.14), $[W/m^2K]$.

$T_{f,i}$ is the surface temperature front side of pane i, $[K]$.

$T_{b,i+1}$ is the surface temperature back side of glazing i+1, $[K]$

T_{cav} is the equivalent mean temperature of the air in ventilated cavity given by equation (2.26), $[K]$

On the inside and outside boundaries of the window the convective heat flow is given by:

$$Q_{c,out} = h_{c,out} A (T_{f,1} - T_{out}) \tag{2.11}$$

$$Q_{c,in} = h_{c,in} A (T_{in} - T_{b,n}) \tag{2.12}$$

Where the convective heat transfer coefficients, $h_{c,out}$ and $h_{c,in}$ is given by table 2.1 on page 12.

2.2.1.1 Convective Heat Transfer Coefficients

The surface to air convective heat transfer coefficient for the cavity is determined by the surface to surface convective heat transfer coefficient $h_{c,i}$ and the average air velocity V, $[m/s]$.

$$h_{cv,i} = 2h_{c,i} + 4V_i \tag{2.13}$$

Where:

$h_{cv,i}$ is the convective heat transfer coefficient for non-ventilated cavities, $[W/m^2K]$.

V_i is the average air velocity in the cavity caused by the ventilation. in the present version of the program it is only possible to calculated with a fixed flow rate, $[m/s]$.

The surface to surface convective heat transfer coefficient h_c is given by:

$$h_c = Nu \left(\frac{\lambda}{d} \right) \tag{2.14}$$

Where d is the thickness of the cavity and λ_g is the thermal conductivity of the fill gas. The Nusselt number, Nu is calculated using correlations based on experimental measurements of heat transfer. Nu is a function of the Rayleigh number, Ra and the cavity aspect ratio, A_g. The Rayleigh number can be expressed as:

$$Ra = \frac{\rho^2 d^2 g \beta C_p \Delta T}{\mu \lambda} \tag{2.15}$$

If the fill gas is treated as a perfect gas, the thermal expansion coefficient of the fill gas, β, is:

$$\beta = \frac{1}{T_{cav}} \qquad [1/K] \tag{2.16}$$

Where T_{cav} is the average temperature for the fill gas in the cavity. The aspect ratio of the i'th fill gas cavity is:

$$A_g = \frac{H}{d} \qquad [-] \tag{2.17}$$

Where H is the height and d the depth of the cavity.

For vertical cavities ISO standard gives the following definition for the Nusselt number:

$$Nu_1 = [Nu_i, Nu_2]_{max} \tag{2.18}$$

where:

$$\begin{aligned} Nu_1 &= 0.0674 Ra^{\frac{1}{3}} && \text{for} \quad 5 \cdot 10^4 < Ra \\ Nu_1 &= 0.0284 Ra^{0.4134} && \text{for} \quad 1 \cdot 10^4 < Ra \leq 5 \cdot 10^4 \\ Nu_1 &= 1 + 1,76 \cdot 10^{-10} Ra^{2.2984755} && \text{for} \quad Ra \leq 1 \cdot 10^4 \end{aligned} \tag{2.19}$$

$$Nu_2 = 0.242 \left(\frac{Ra}{A_g} \right)^{0,272} \tag{2.20}$$

2.2.2 Advective Heat Flux

The advective heat flux to the cavity by ventilation, Q_{adv}, depends on the air flow rate as well as the temperature difference between the incoming and outgoing air.

$$Q_{adv} = Q_{adv,out} - Q_{adv,in} = \rho c_p \varphi_v (T_{cav,in} - T_{cav,out}) \qquad [W] \tag{2.21}$$

Where:

ρ is the density of the gas in the cavity at temperature T_{gap}, $[kg/m^3]$.

φ is the volumetric air flow rate in the cavity, $[m^3/s]$.

Q_{adv} is not to be confused with the ventilation heat loss, Q_{vent}. While Q_{adv} is the advective heat flux to the cavity, Q_{vent} is the advective heat flux to the indoor room. $Qvent$ is the energy needed to warm the ventilation air to indoor temperature.

$$Q_{vent} = \rho c_p \varphi (T_{out} - T_{in}) \qquad [W/m^2] \tag{2.22}$$

The air flow is given as volume flow $[m^3/s]$, which could imply a constant volume flow. But for a steady state situation there must be a constant mass flow – not a constant volume flow. Therefore the density ρ, heat capacity c_p and volume flow φ have to be given for the same temperature. As a standard the indoor temperature T_{in} is used because the volume flow then compares to the exhaust volume flow.

2.2.3 Temperature in Cavity

In order to calculate the convective heat flows in the cavity, $Q_{cv,f,2}$, $Q_{cv,b,1}$ and the advective heat flow, Q_{adv} is it necessary to know both the cavity air temperature, T_{cav} and the temperature of the air leaving the cavity, $T_{cav,out}$. The temperatures are calculated with an analytical expression that considers only the vertical temperature variation.

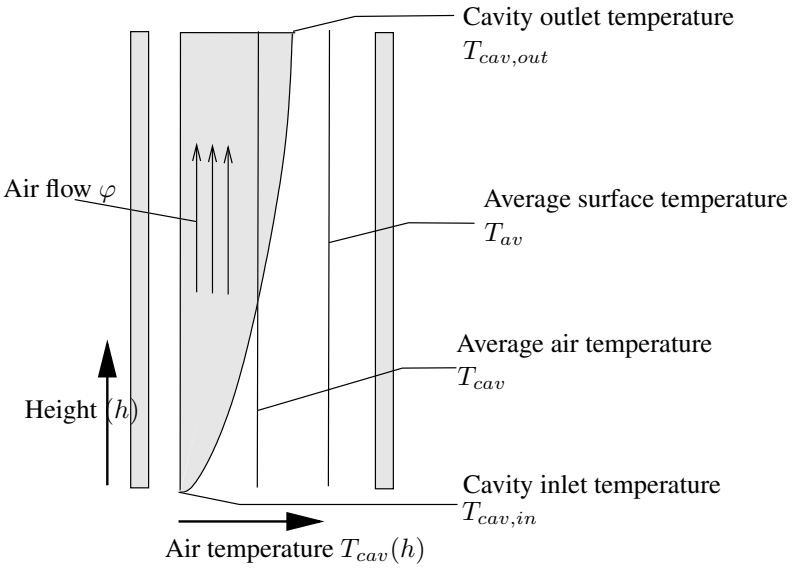

FIGURE 2.4: *Temperature profile of air in ventilated cavity*

The air temperature as function of the height is calculated by:

$$T_{cav}(h) = T_{av} - (T_{av} - T_{cav,in}) \cdot e^{-h/H_0} \tag{2.23}$$

Where:

H_0 is the characteristic height or temperature penetration length given by equation (2.25).

T_{av} is the average temperature of the surfaces to the cavity.

It follows that the temperature of the air leaving the cavity is given by:

$$T_{cav,out} = T_{av} - (T_{av} - T_{cav,in}) \cdot e^{-H/H_0} \tag{2.24}$$

For known volume flow is the characteristic height, H_0 given by:

$$H_0 = \frac{\rho \cdot c_p \cdot d}{2h_{cv}} \cdot V \tag{2.25}$$

Where:

d is the width of the cavity [m].

V is the velocity of the air flow in the cavity [m/s].

The volume average temperature of the air in the cavity can then be found by integrating over the height of the cavity.

$$T_{cav} = \frac{1}{H}\int_0^H T_{cav}(h) \cdot dh = T_{av} - \frac{H_0}{H}(T_{cav,out} - T_{cav,in}) \tag{2.26}$$

2.2.4 Conduction in Glass Panes

The conductive heat flow through the pane depends on the thermal conductivity of glass. Like for the convective heat flow in the ventilated cavity the subscriptions (f), (m) and (b) are used to indicate respectively the front, middle or back of the pane(i).

$$Q_{g,f,i} = A\frac{2\lambda_g}{d} \cdot (T_{m,i} - T_{f,i}) \tag{2.27}$$

Where:

Q_g is the conductive heat flow in the glass pane $[W]$.

λ_g is the thermal conductivity of glass $[W/mK]$.

d is the thickness of the pane $[m]$.

The heat flow in the glass is split in two, front side $Q_{g,f}$ and back side $Q_{g,b}$.

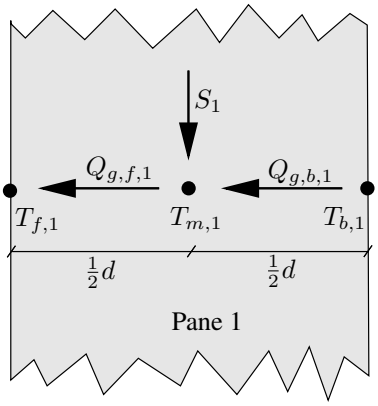

FIGURE 2.5: *Numbering system for the conductive heat transfer*

The sun energy absorbed by the glass S_i is applied to the middle temperature node.

2.2.5 Radiative Heat Transfer

The longwave radiative heat transfer between the glass panes is describes by one dimensional relations. Since glass is completely opaque to infrared radiation the transmission through the panes is removed from the equations as they are presented by ISO standard. To ease the calculations the wavelength dependent properties are not considered. The radiosities between to opposite

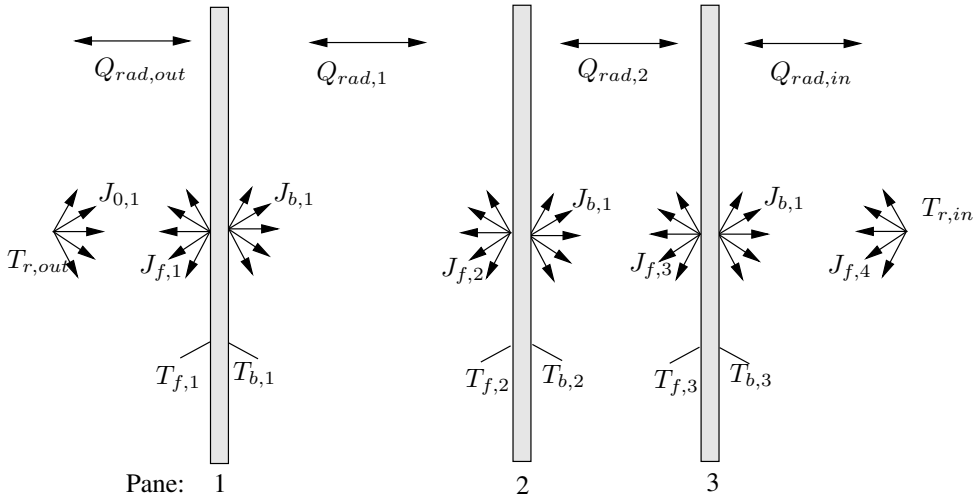

FIGURE 2.6: *Numbering system for the radiative heat transfer*

panes are given by:

$$J_{f,i} = \varepsilon_{f,i} \cdot \sigma \cdot T_{f,i}^4 + \rho_{f,i} \cdot J_{j,i-1} \tag{2.28}$$

$$J_{b,i-1} = \varepsilon_{b,i-1} \cdot \sigma \cdot T_{b,i-1}^4 + \rho_{b,i-1} \cdot J_{f,i} \tag{2.29}$$

The radiative heat flow is the difference between the radiosities

$$Q_{rad,i} = A \cdot (J_{f,i} - J_{b,i-1}) \tag{2.30}$$

Solving the two radiosity equations with two vairables give:

$$J_{f,i} = \frac{\varepsilon_{f,i} \cdot \sigma \cdot T_{f,i}^4 + \rho_{f,i} \cdot \varepsilon_{b,i-1} \cdot \sigma \cdot T_{b,i-1}^4}{1 - \rho_{f,i} \cdot \rho_{b,i-1}} \tag{2.31}$$

$$J_{b,i-1} = \frac{\varepsilon_{b,i-1} \cdot \sigma \cdot T_{b,i-1}^4 + \rho_{b,i-1} \cdot \varepsilon_{f,i} \cdot \sigma \cdot T_{f,i}^4}{1 - \rho_{b,i-1} \cdot \rho_{f,i}} \tag{2.32}$$

Where:

ε is the longwave emissivity of the front ($_f$) or back ($_b$) side of pane i.

σ is Stefan-Boltzmann constant $5.67 \cdot 10^{-8}$, $[W/mK]$

ρ is the long wave reflectance of the front ($_f$) or back ($_b$) side of pane i.

The effects of the boundaries are included by setting:

$$J_{f,n+1} = \sigma \cdot T_{r,in}^4 \tag{2.33}$$
$$J_{b,0} = \sigma \cdot T_{r,out}^4 \tag{2.34}$$

$t_{r,in}$ is the mean radiation temperature of the indoor environment.

$t_{r,out}$ is the mean radiation temperature of the outdoor environment.

2.2.6 Solar Irradiation

The solar transmittance of the window and the absorbed solar energy is calculated in accordance with ISO standard Annex A, *Solution technique for the multi-layer solar optical model*, [11]. As for radiative heat transfer, no wavelength dependent properties are included.

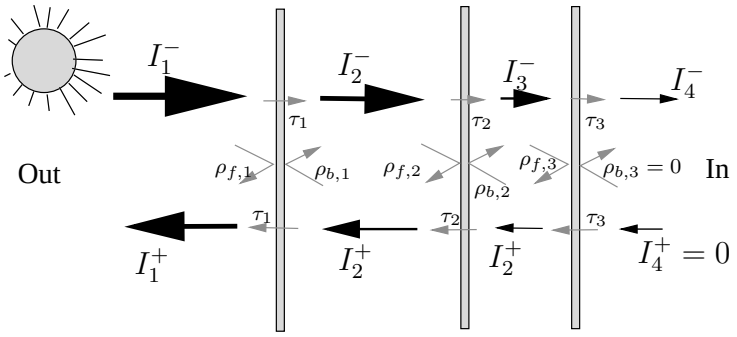

FIGURE 2.7: *Numbering system for the solar heat flux*

$$I_i^+ = \tau_i I_{i+1}^+ + \rho_{f,i} I_i^- \quad \text{for } i = 1 : n+1 \tag{2.35}$$
$$I_i^- = \tau_{i-1} I_{i-1}^- + \rho_{b,i-1} I_i^+ \quad \text{for } i = 2 : n+1 \tag{2.36}$$

Where:

I is the solar radiation in a given direction

τ_i is the solar transmittance for pane i

ρ is the solar reflectance for the given surface

The ratio, r_i, between radiation in opposite direction, I_i^+ andI_i^- is given by:

$$\frac{I_i^+}{I_i^-} = r_i = \rho_{f,i} + \frac{\tau_i^2 r_{i+1}}{1 - \rho_{b,i} r_{i+1}} \tag{2.37}$$

and the ratio between radiation in the same direction but in cavities next to each other are given by:

$$\frac{I_{i+1}^-}{I_i^-} = t_i = \frac{\tau_i}{1 - \rho_{b,i} r_{i+1}} \tag{2.38}$$

The reflectance of the indoor environment is set to zero and so I_4^+ are also zero. Therefore the r-ratios can be calculated using equation (2.37). Knowing the r-ratios the t-ratios can be calculated. The incident solar radiation I_1^- does not need to be known, and is just set to unity, for these calculations. Now the radiation reflected to the outdoor side can be calculated using:

$$I_1^+ = r_1 \cdot I_1^+ \tag{2.39}$$

moving towards the indoor side from $i = 2$ to $i = 4$ the remaining radiation fluxes can be calculated

$$I_i^- = t_{i-1} \cdot I_{i-1}^- \quad \text{and} \quad I_i^+ = r_i \cdot I_i^- \tag{2.40}$$

The amount of incident solar radiation absorbed at each layer, S_i, can then be calculated as:

$$S_i = A_i \cdot I_s \tag{2.41}$$

Where:

$$A_i = \frac{I_i^- - I_i^+ + I_{i+1}^+ - I_{i+1}^-}{I_1^-} \tag{2.42}$$

2.2.7 Thermophysical Gas Properties

The thermophysical properties of the gas in the cavities are determined in accordance with ISO standard Annex B.

Thermal conductivity, $\lambda = a + b \cdot T \quad [W/mK]$

gas	coefficient a W/mK	coefficient b W/mK^2	λ at $0°C$ W/mK	λ at $10°C$ W/mK
air	$2.78 \cdot 10^{-3}$	$7.76 \cdot 10^{-5}$	0.024	0.025
argon	$2.29 \cdot 10^{-3}$	$5.15 \cdot 10^{-5}$	0.016	0.017
krypton	$0.94 \cdot 10^{-3}$	$2.83 \cdot 10^{-5}$	0.0087	0.009

Viscosity, $\mu = a + b \cdot T \quad [N \cdot s/m^2]$

gas	coefficient a $N \cdot s/m^2$	coefficient b $N \cdot s/m^2$	μ at $0°C$ $N \cdot s/m^2$	μ at $10°C$ $N \cdot s/m^2$
air	$3.72 \cdot 10^{-6}$	$4.94 \cdot 10^{-8}$	$1.72 \cdot 10^{-5}$	$1.77 \cdot 10^{-5}$
argon	$3.38 \cdot 10^{-6}$	$6.455 \cdot 10^{-8}$	$2.10 \cdot 10^{-5}$	$2.16 \cdot 10^{-5}$
krypton	$2.21 \cdot 10^{-6}$	$7.78 \cdot 10^{-8}$	$2.40 \cdot 10^{-5}$	$2.42 \cdot 10^{-5}$

Specific heat capacity, $C_p \quad [N \cdot s/m^2]$

gas		C_p at $0°C$	C_p at $10°C$
air	$C_p(T) = 1039 - 0.255T + 0.000485T^2$	1006.0	1006.1
argon	constant	521.9	521.9
krypton	constant	248.1	248.1

TABLE 2.2: *Calculation of thermophysical constants*

Chapter 3

Description and Validation of CFD Models

This chapter contains a detailed description of the CFD model. The model is validated by grid dependency analysis and comparison to ISO standard calculations for closed cavity.

3.1 Geometry and Boundary Conditions

The CFD model is limited to the ventilated cavity of the air flow window. The boundaries of the model are the panes and frame enclosing the cavity.

3.1.1 Geometry

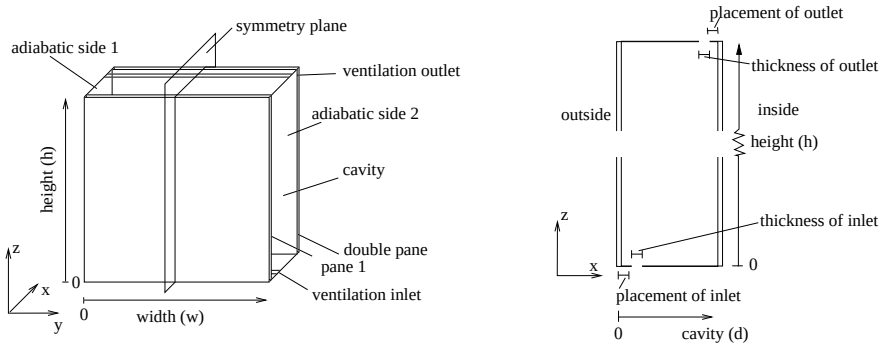

FIGURE 3.1: *Dimension of air flow window cavity*

The window cavity is for the reference case 0.05 m deep, 1 m wide and 1 m high, figure 3.1. The inlet is placed at the bottom as a 5 mm wide slit in

the whole width of the window placed 5 mm from the outside boundary. The outlet is like the inlet, but placed in the top, 5 mm from the inside boundary.

There is a geometrical symmetry plane. If the flow is almost symmetrical it is possible to cut the computational domain in half by implementing a symmetry boundary condition. This would greatly decrease the computational time. A simulation of the reference case boundary conditions, see section 3.1.2, was conducted for the complete domain and the symmetry of the flow investigated. The temperature distribution is very symmetrical as shown in figure 3.2. But to make sure the flow is symmetrical the velocities normal to the symmetry plane is investigated.

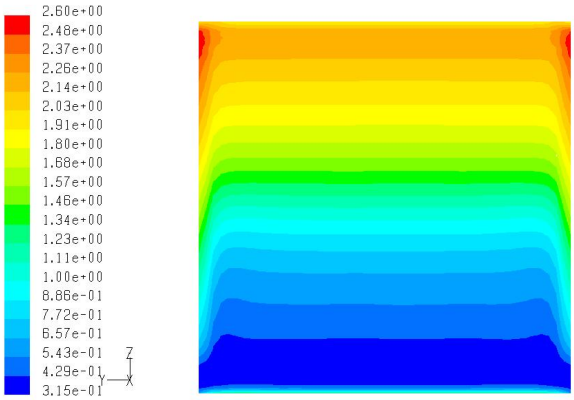

FIGURE 3.2: *Contours of temperatures [°C] in the width. Middle of cavity, plane* $x = 0.025$.

Contour plots of the overall velocity magnitude and the velocity normal to the geometrical symmetry plane are shown in figure 3.3 on the next page and 3.4 on the facing page. The average velocity for the geometrical symmetry plane is $6.4{\cdot}10^{-2}\ m/s$. The velocity normal to the symmetry plane is much smaller, with an maximum absolute velocity of $2.3 \cdot 10^{-4}\ m/s$. (The normal velocity is directional and can be both positive and negative.) The velocities in the symmetry plane are more than 100 times larger than velocities normal to symmetry plane. It can therefore be assumed that the flow is symmetrical and symmetry boundary conditions can be applied at the geometrical plane of symmetry.

3.1.2 Boundary conditions

The boundaries of the computational domain consist of the inside and outside panes, the top, bottom and side of the cavity and the ventilation inlet and outlet slits placed respectively in bottom and top of the cavity. An overview of the boundary conditions are given in table 3.1 on the next page

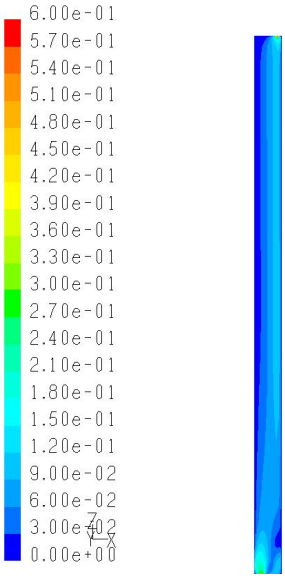

FIGURE 3.3: *Velocity magnitude contour plot at geometrical symmetry plane [m/s]. There is a factor 1000 difference between the scale in this figure and in figure 3.4.*

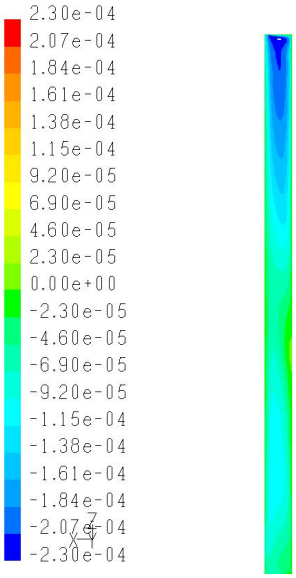

FIGURE 3.4: *Contour plot of velocity normal to symmetry plane at the geometrical symmetry plane [m/s]. The scale has both negative and positive values because the velocity has direction.*

	Type	Setting	Emissivity
Adiabatic walls	heat flux	0 W/m^2	0
Outside pane	convection	18 W/m^2K	0.9
Inside pane	convection	1.72 W/m^2K	0.9
Inlet	velocity inlet	0.6 m/s - 0 °C	0
Outlet	outflow	[-]	0
Symmetry	symmetry	[-]	[-]

TABLE 3.1: *Boundary conditions.*

Adiabatic sides. It is generally accepted to distinguish between the U-value of the pane area, centre U-value, and the thermal linear transmittance, that is the multi dimensional heat flows caused by spacer or frame. This project is limited to the pane area of windows. Therefore effects of spacer or frame separating the panes are not inlcuded. The heat flows through the bottom, top and sides are any way expected to be small compared to the heat flows through the panes. On theses sides therefore adiabatic wall boundary conditions are imposed.

Panes. The heat flows through the panes are in return very important. But neither the surface temperature nor the heat flux is known in advance, and the distribution, especial vertical, of the surface temperature and heat flux is one of the main aims of the simulations. It is therefore not possible to impose an arbitrary surface temperature or heat flux. The air temperature at the indoor and outdoor conditions are the only knowns. It is therefore chosen to impose a wall boundary with convective resistance. This has the effect that when calculating the one-dimensional heat flux through the pane, there is included a resistance on the external (to the computational domain) side of the panes. The convective resistances imposed are in accordance with the reference boundary conditions given by the ISO standard.

The solar absorption in the panes are simulated by giving the boundary wall a thickness and an internal heat generation. The heat fluxes through the panes are solved one-dimensionally.

Inlet and Outlet. A fixed flow rate is wanted for the CFD simulations. The boundary condition of the ventilation inlet is therefore a fixed velocity. It is assumed that there is a uniform distribution of inlet air in the width of the window. The outlet is assumed to have no effect on the cavity and is therefore simulated as a simple outflow boundary.

Symmetry. As discussed above the computational domain is cut in half by imposing a symmetry boundary on the geometrical plane of symmetry. A symmetry boundary simple imposes that no flux can exist through the boundary.

Radiation. The influences of the adiabatic boundaries on the radiation are excluded by setting the emissivity factor of these surfaces to zero. The emissivities of the panes are set to 0.9, which is roughly equal to an uncoated pane.

3.2 Mesh Generation

The geometry and mesh is created in the Gambit program package. The domain is meshed by first linking adiabatic side 1 and 2 and then meshing the faces on the sides. Then the Cooper method is used to mesh the volume.

The faces on the adiabatic side 1 and 2 are meshed by use of a size function attached to the inlet and outlet edges and a boundary layer attached to the edge of the inside and outside faces. The size function is attached to the adiabatic

side 1 and side 2 faces with sources on the edge of inlet and outlet face. The initial size is set to 0.5 mm to ensure a high number of cells in the inlet and outlet gap. The growth factor is set to 1.1 to ensure that the cells increase in size quite slowly. The size limit is set to 2.5 mm. The boundary layer is attached to the edges of the inside and outside faces to ensure a refined mesh close to the inside and outside panes. The width of the first layer is set to 0.5 mm and the growth is set to 1.115 for 7 rows. The volume is then meshed with the cooper method using a distance of 10 mm. See also table 3.2 on page 29 in section 3.2.2 *Grid Dependency Analysis*. The mesh near the inlet opening is shown in figure 3.5.

This method of meshing creates some cells with high aspect ratios near the inlet and the outlet and at the boundary layers. In the boundary layer the flow direction is mainly in the (y,z)-plane, parallel to the boundary. Near the inlet and outlet there is close to no velocity in the y-direction. The high aspect ratios should therefore not cause any problems.

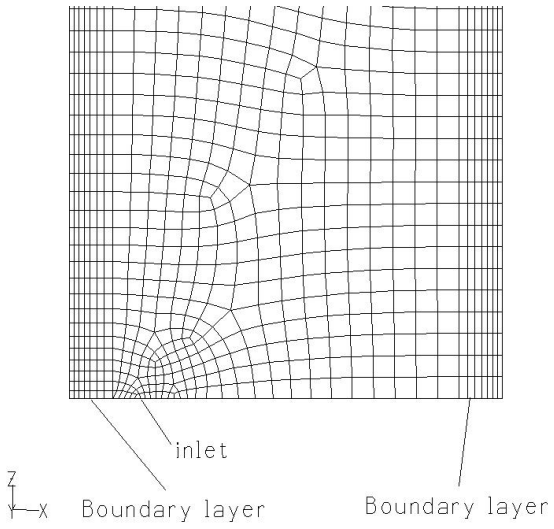

FIGURE 3.5: *Detail of mesh close to the inlet opening.*

3.2.1 Near Wall Treatment

The velocity profile near walls can be very steep and for turbulent flows the prediction of near-wall phenomena are very dependent on wall functions and the near-wall mesh. Wall functions are used with coarse near-wall mesh to provide sufficient boundary conditions for turbulent flows. The near-wall mesh can be characterized by the placement of the first grid point, expressed

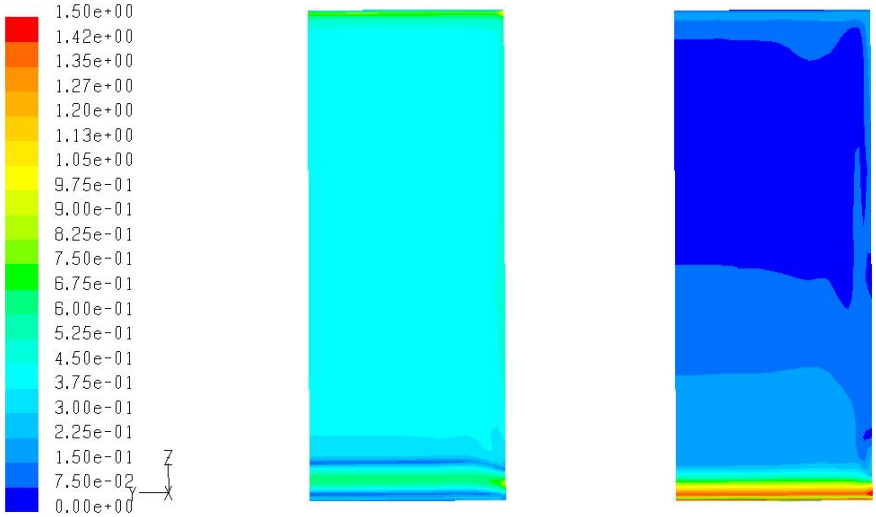

FIGURE 3.6: *Contour plot of y^+-value at inside pane, left, and outside pane, right.*

by the y_p^+-value [16].

$$y_p^+ = \frac{y_p \cdot u_\tau}{\nu} \tag{3.1}$$

Where:

y_p is the distance from the wall to the first grid point.

u_τ is the velocity component parallel to the wall.

ν is the viscosity.

It is generally accepted that for $y_p^+ < 5$ the grid point can be assumed to be located in the laminar viscous sublayer [16], so that that the boundary layer is adequately meshed and no wall functions are required. For all wall boundaries, except the adiabatic narrow side, the first grid point is placed so close to the wall, that $y_p^+ < 2$, se figure 3.6. The largest y^+-values are found on the lower part of the outside pane where the inlet jet causes high velocities near the surface.

No boundary layer is implemented on the adiabatic sides, so the first grid point is located much father from the wall. This gives y^+-values somewhat higher in the range of $2 < y^+ < 5$. Expect for small regions in top and bottom near inlet and outlet with high near wall velocities. But this is acceptable because these near wall flows are not so important since there isn't any heat flux through these faces.

Since no complex near-wall flows like swirls are expected the standard wall function is used. The standard wall function implements the "log-law", that assumes logarithmic relationship between distance and velocity. But for the $y_p^+ < 13$ the standard wall function by default omits the "log-law" because the near wall grid is assumed fine enough to resolve the viscous sublayer. This means that that for the majority of wall boundaries and on all wall boundaries with convective heat fluxes no wall function is used.

3.2.2 Grid Dependency Analysis

The grid dependency is investigated by conducting simulations for the reference case with an increasing number of cells. The grid adaption function in FLUENT can not be used together with the DTRM radiation model. The refinement/coarsening of the grid is therefore conducted by applying a factor to the mesh generation parameters mentioned in section 3.2 on page 26. This grid factor is varied between 0.7 and 2.0 producing between $56\,000$ and $1\,5\,000$ cells, see table 3.2.

grid factor		0.7	1.0	1.5	2.0
size function	initial size $[mm]$	0.35	0.50	0.75	1.0
	growth factor $[-]$	1.1	1.1	1.1	1.1
	size limit $[mm]$	1.75	2.5	3.75	5
boundary layer	first layer $[mm]$	0.35	0.50	0.75	1.0
	growth factor $[-]$	1.115	1.115	1.115	1.115
Cooper method	distance $[mm]$	7	10	1.5	20
number of cells		1 490 929	306 225	193 809	56 150

TABLE 3.2: *Parameter variation for grid dependency analysis.*

The results of the grid variation study are plotted in figure 3.7 on the next page. There is very little variation of the resulting convective heat flux and preheating for grid factor 0.7 to 1.5. It can therefore be concluded that the results are grid independent for the reference case mesh, with a grid factor of $1.0 \approx 300\,000$ cells.

3.3 Turbulence Model

It is often proposed by textbooks like the FLUENT manual [16], that the flow regime for natural convection in closed domain can be characterized by the Rayleigh number. Rayleigh numbers less than $Ra < 10^8$ in-

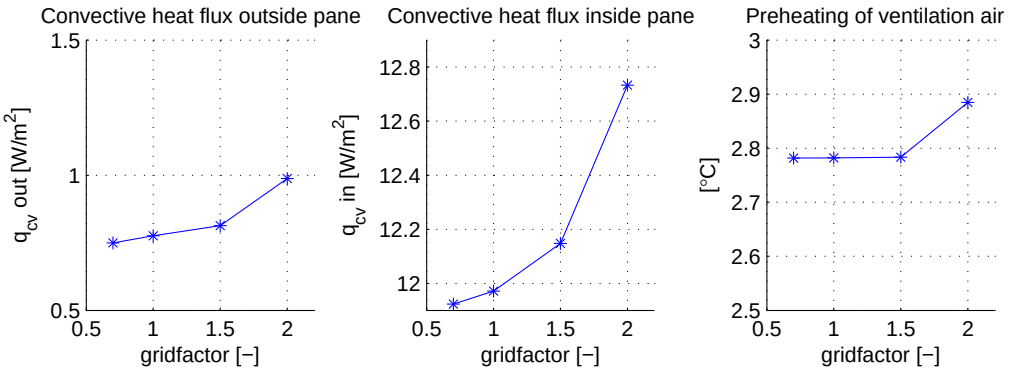

FIGURE 3.7: *Results of grid dependency analysis.*

dicate laminar flow, with transition to turbulence occurring over the range of $10^8 < Ra < 10^{10}$. Closed vertical cavities are very important for heat transfer in windows and wall cavities. So this particular geometry has been the subject of many numerical and experimental studies. In 1978 Yin [17] proposed a relationship between the aspect ratio, Rayleigh number and flow regime as shown in figure 3.8. For a more comprehensive literature study see [18] or [19].

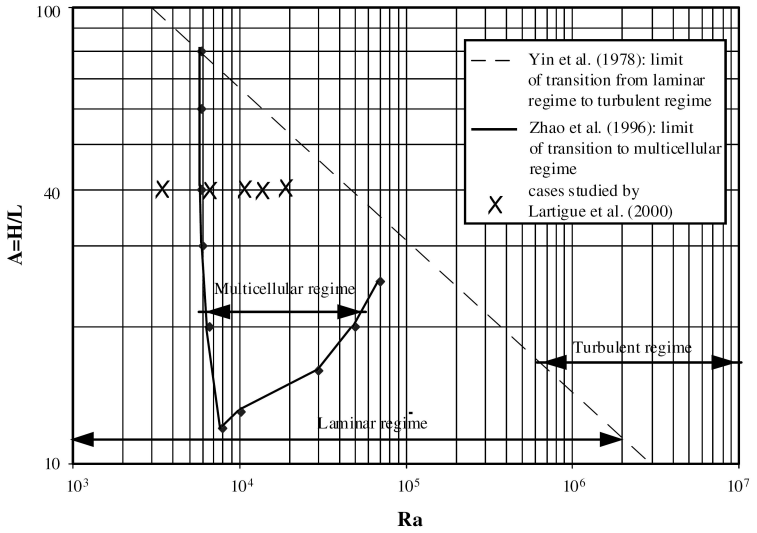

FIGURE 3.8: *Flow regimes definitions for natural convection in vertical enclosures [20]*

But even in laminar flow regimes the flow is not always easily predictable because of occurrence of multicellular flows. Multicellular flows are characterized by many smaller vortices and not just one large vortex covering the whole enclosure. Previous work by [18, 20, 21] have showed that the development of multicellular flow is important for the heat flow, but that these developments are difficult to predict with steady state laminar models. [19] recommend to use the renormalisation group k-ϵ model because of its ability to cover flow regimes from laminar to turbulent.

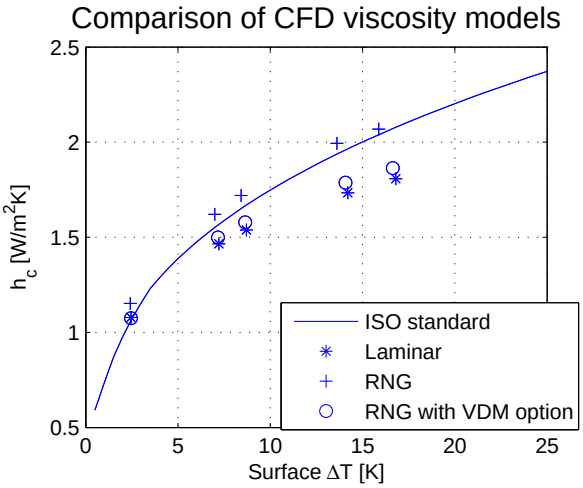

FIGURE 3.9: *Convective heat transfer coefficient for unventilated cavity. Comparison of ISO standard method and CFD simulations with different turbulence models. RNG is renormalisation group $k-\epsilon$ model. VDM option is Viscosity Differential Model.*

The turbulence models is verified by comparison of the resulting convective heat transfer coefficients, h_c. The validation is conducted for a closed vertical cavity – the geometry of the reference model but without ventilation. For reference data is used the ISO standard [11] calculation of h_c.

Convective heat fluxes are the main aim of the CFD modelling, as well as being a parameter closely linked to both the near wall effects and the overall flow pattern. Convective heat transfer coefficients are, for unventilated cases, a convenient simplification of convective heat fluxes. The results of the validation are shown in figure 3.9. The convective heat transfer coefficient is calculated by:

$$h_c = \frac{q_c}{\Delta T} \tag{3.2}$$

Where:

q_c is the convective heat transfer across the cavity.

ΔT is the difference between the average surface temperatures of the opposing surfaces. Not to be confused with the inside and outside temperatures. It is the same surface temperatures that are used in ISO standard calculation of h_c presented in section 2.2.1.1

From the results of the verification plotted in figure 3.9 on the preceding page, it can be seen that the standard renormalisation group (RNG) model has the overall best fit with the ISO standard. The only exception is for the smallest surface temperature difference of $\Delta T \approx 2.5$. But according to [17] this flow is laminar and far from the turbulence transition zone and according to [18, 20, 21] without multicellular flows. So it is not so surprising, that the laminar model shows the best result.

When ventilation of the cavity is implemented the flow is expected to become more turbulent because of the inlet jet and the overall higher velocities. The renormalisation group (RNG) turbulence model is therefore chosen.

The standard k-ϵ model was also tried. But it did not easily produce convergence and the results were way off compared to the ISO standard.

3.3.1 Solver Execution

The solver implemented is a segregated implicit solver with first order upwind discretization for momentum, turbulent kinetic energy, turbulent dissipation rate and energy. The natural buoyancy is resolved by use of the Boussinesq approximation.

Fluent default values are used for under-relaxation factors, 3.3.

Under-relaxation factor	value
Pressure	0.3
Density	1
Body forces	1
Momentum	0.7
Turbulence kinetic energy	0.8
Turbulence dissipations rate	0.8
Turbulent viscosity	1
Energy	1

TABLE 3.3: *Under-relaxations factors*

3.4 Radiation Model

Radiative heat fluxes play a important role in normal windows. But in a ventilated cavity the temperature difference between the surfaces can be much larger than otherwise and the radiative heat exchange between panes plays a dominating role. It is therefore crucial to include the radiative heat fluxes in the CFD simulations.

The best radiation model for enclosed spaces and were the fluid doesn't partake in the radiation, like our ventilated cavity, is properly the Surface to Surface model. The Surface to Surface model is a view factor model and calculates the view factor between all surfaces in the domain. But calculating the view factors is a large operation and the computer resources available could not handle this task. The computational domain simply had too many boundary surfaces. The implemented radiation model is instead the Discrete Transfer Radiation Model (DTRM), which is basically a ray tracing model. But the DRTM model can only achieve radiation energy balance if the participating faces have equal surface emissivities. The participation of the air is omitted by setting the absorption coefficient to zero.

3.5 Convergence

In order to check if and when the simulations have reached convergence both residuals and the energy balance for the computational domain are monitored. Convergence is achieved when the simulations have reached a stable steady state solution, that doesn't change even if many more iterations are performed.

Generally a decrease by 3 orders of magnitude for the residuals is accepted as appropriate convergence criterion. But it turns out that for the RNG k-ϵ turbulence model this does not guarantee stable solutions. Therefore the residuals convergence criteria, listed in 3.4 on the following page, are set much lower. Additionally a minimum of 1000 iterations are enforced to be sure that the solution is stable.

In figure 3.10 on the next page the residual history for a representative case may be seen. A stable solution is reached after approximately 700 iterations and convergence is achieved.

To ensure energy balance is achieved the combined heat flux of all the boundaries are monitored along with monitoring of the residuals.

Residual	Criterion
Continuity	1e-05
x-velocity	1e-05
y-velocity	1e-05
z-velocity	1e-05
Energy	1e-07
k	1e-06
ϵ	1e-06

TABLE 3.4: *Settings of the residuals convergence criteria.*

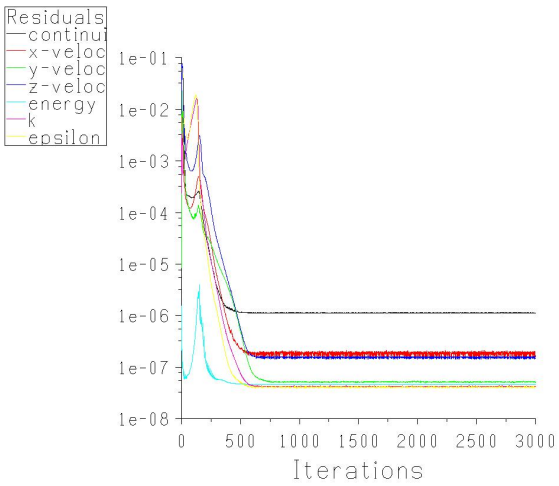

FIGURE 3.10: *Convergence history of residuals. RNG k-ϵ turbulence model.*

3.6 Conclusion

The main drawback of using CFD-modeling as the tool of analysis and omitting experimental test, is the difficulty of validation. By its very nature CFD-modeling can never give the exact result, only a good approximation. So without real testing to validate against, it is difficult to know whether the CFD model calculates correctly – on the scale needed. The CFD model is therefore validated against a well known and extensively researched case: natural convection in a closed vertical cavity.

Comparison with the ISO standard method for closed cavities has shown that the ReNormalisation Group (RNG) turbulence model has the overall best results. But for low surface temperature differences, where the flow is expected to be laminar and without multi cellular flows, the laminar or the RNG-model with Viscosity Differential Model (VDM) enabled, produces the best

results. It is assumed that applying ventilation only increase the turbulence and it is therefore chosen to use the RNG turbulence model for the simulations.

The grid dependency analysis has shown that refinement of the grid will only cause minor changes to the results. It is therefore reasonable to assume grid independency of the simulations.

The results of the simulations are presented in the next chapter.

Chapter 4

CFD Simulation Results

The purpose of the CFD simulations is to analyze the relationship between the specific geometry, conditions and the convective heat fluxes in the cavity. Based on a reference case a range of parameter variations of geometry and conditions are conducted. The reference case is a 1 m high cavity, a depth of 50 mm, ventilation volume flow of 3 l/s, a temperature difference between inside and outside of 20 $^{\circ}C$ and no solar irradiation.

The ventilation flow depends on the pressure difference across the window. But the cause of the pressure difference is of no particularly interest for the air flow pattern. It is the aim of this project to present a method for calculating the thermal performance for specific conditions. How the conditions are achieved is not important for the thermal performance of the window and is as such outside the scope of the project.

As mentioned above does this project not deal specifically with how the air flow through the window is achieved. But in real situations the airflow can be achieved by exhaust ventilation or by some kind of natural ventilation. If the ventilation flow depends on wind induced pressure differences, the air flow speed will of cause much more likely be fluctuating, and the direction (in- or outwards) can not easily be controlled. But CFD analysis of transient and changing boundary conditions is very time consuming. So because of the need to limit the scope of this analysis it is chosen not to investigate the significance of fluctuating airflow speeds due to changing wind pressure. It is assumed that for the dominating time periods the wind pressure (if any) is stable enough to cause stable airflows inside the window. For situations with exhaust ventilation the pressure difference caused by the mechanical exhaust will in most cases be much higher than the wind driven, rendering the influence of wind negligible.

4.1 Parameter Studies

The parameters expected to influence the air flow pattern and the convective heat flow is the specific geometry, ventilation flow and outside conditions.

Ventilation rate. The ventilation volume flow is varied between 1 and 15 l/s per meter width of the window. Corresponding to an average velocity in the cavity between 0.02 and 0.3 m/s. The range is chosen so that the convection is dominated by natural buoyancy for the lowest ventilation rates and that the natural buoyancy is negligible for the highest ventilation rates.

Solar irradiation. The surface temperatures of the cavity are increased by applying internal heat generation to the pane boundaries. The internal heat generation corresponding to an absorption of 12% in the outside pane and 10% in the inside pane of the total solar irradiation. The absorption is evenly spread out over the entire pane and any effects of shades cast by the frame are not included. The solar irradiation is varied between 0 and 1000 W/m^2.

Cavity depth. The depth of the cavity effects both the average velocity of forced air flow and thermal resistance of the cavity. The cavity depth is varied between 50 and 150 mm.

Window height. The height of the window determines how long it takes for the air to flow through the cavity. The higher the cavity the higher the potential preheating of the air. The height is varied between 0.75 and 1.5 m.

4.2 Simulation Results

The CFD simulations including solar irradiation can not adequately be transformed directly to performance parameters for windows. The simplification of effect of solar irradiation on the boundaries gives rise to large uncertainties concerning the resultant solar transmission. Therefore the CFD results are only reported for the ventilated cavity and not the as resultant performance for the whole window. The analyses are, like the results, limited to the cavity. The surface temperatures found by the CFD simulations are used as boundary conditions for the analyses of calculation methods.

Since the authorized method is the existent ISO standard method, the results are shown together with the corresponding ISO standard heat flows calculated from the average surface temperatures.

The main results from the CFD simulations are reported as:

- Convective heat flux through surfaces
- Temperature increase of ventilation air

For visualizing the flow pattern, temperature and velocity profiles are made, by plotting the temperature respectively the velocity in upwards direction through the cavity (depth). The profiles are made for every 10 cm vertically. Profiles for all cases are located in appendix A.

The radiative heat flux is, as expected, very well described by the ISO 15099 standard. The differences between the ISO standard and the CFD calculations are less than 2%.

4.2.1 Dependency on Ventilation Rate

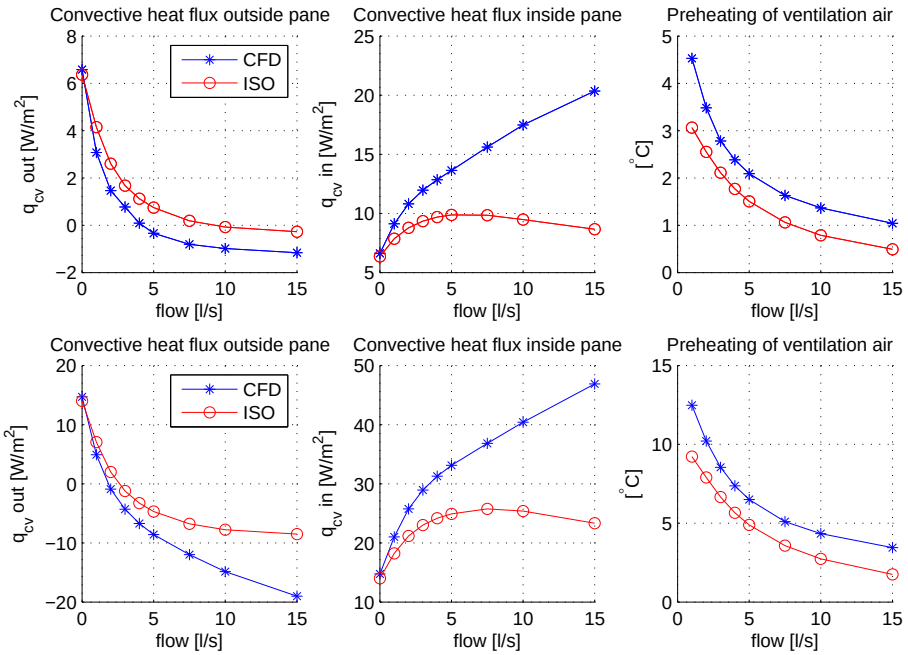

FIGURE 4.1: *Dependency on ventilation flow rate. Comparison of main results from CFD simulations with out solar irradiation, top, and with 500 W/m^2 solar irradiation bottom and corresponding ISO standard calculations*

The main parameter for the convective heat flux is expected to be the ventilation rate and secondly the surface temperature increase caused by solar irradiation. The first parameter study is therefore the ventilation rate, ranging from 1 to 15 l/s per meter width of window.

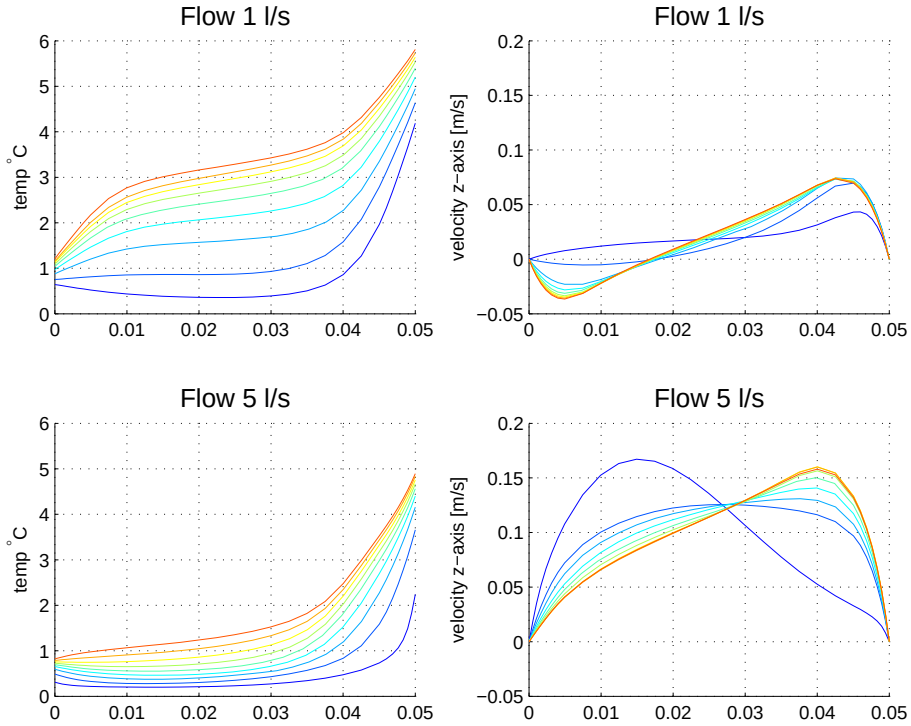

FIGURE 4.2: *Temperature and velocity profiles for cases with 1 and 5 l/s flow and no solar irradiation. Outside is located to the left and inside is located to the left.*

The convective heat fluxes are plotted as a function of ventilation flow rate in figure 4.1 on the preceding page. The heat convective heat flux through the outer pane becomes negative as the ventilation rate is increased. Negative heat flux is a flux in direction from outside to inside. So heat is flowing from the outer pane to the air in the cavity. Even for the case of no solar irradiation, the radiative heat flux from the inner to the outer surface is enough to heat the pane to temperatures above outdoor air temperature. For moderate to high ventilation rates the air in the cavity is very close to outdoor air temperature and is therefore colder than the outer pane and a negative heat flux occurs. This phenomenon can be visualized by temperature and velocity profiles in figure 4.2.

There are significant discrepancies, both in magnitude and in tendency between the CFD results and the ISO standard calculation for the convective heat flows. The CFD simulations show that the convective heat fluxes through the inside surface keep increasing with increased ventilation rate, but this is not monotonically so for the ISO standard.

The velocity profiles are dominated by natural buoyancy at the low ventilation flow of 1 l/s. For a moderate ventilation flow of 5 l/s the velocity pro-

files are a combination of forced flow with symmetrically profiles, and natural buoyancy. The temperature profiles show that for moderate ventilation flow the temperature increase of the cavity air is almost completely confined to an area close to the warm inner pane. This explains why a relative small temperature increase of the outer pane can cause a negative convective heat flux between the cavity and the outer pane.

The placement of the inlet to the cavity close to the outer pane seems only to influence the lowest 10-20 cm of the window. The inlet jet looses momentum after 10-20 cm and the natural buoyancy of the heated air along the inner pane displaces the velocity profile towards the inner pane.

4.2.2 Dependency of Surface Temperatures

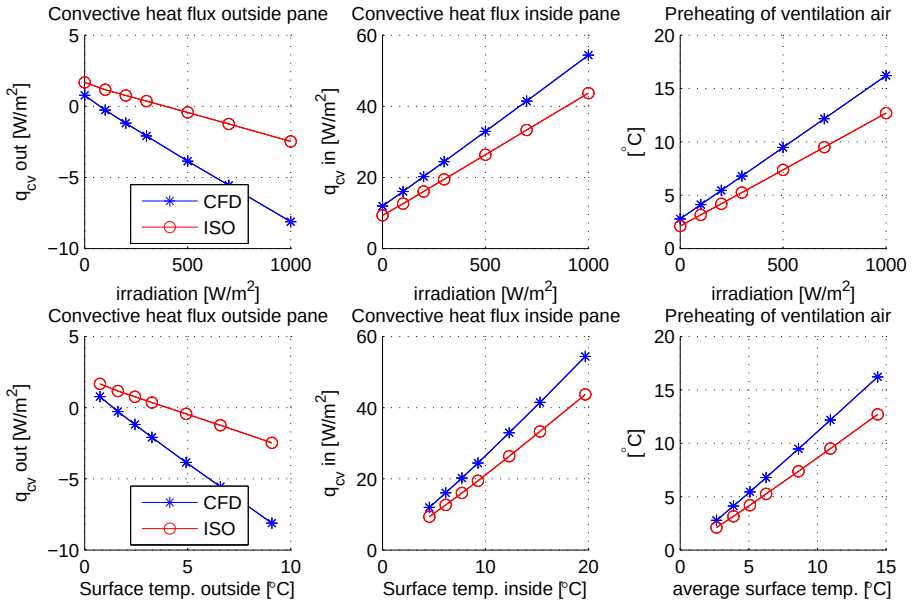

FIGURE 4.3: *Dependency on solar irradiation top, and resulting surface temperatures bottom. Comparison of main results from CFD simulations with solar irradiation and corresponding ISO standard calculations*

Increased surface temperatures are achieved by applying solar irradiation to the panes. The heat flows dependency on surface temperatures is shown in figure 4.3. There is a very linear relationship between the solar irradiation and the heat flows. The linear relationships persist whether the heat flows are plotted as function of solar irradiation or the resulting surface temperatures. The velocity profiles in figure 4.4 on the next page show that the flow pattern is much more dominated by natural buoyancy for case with high solar irradi-

ation. This suggest that the heat flows are not very dependent on the type of flow pattern, but more dependent on the temperature difference between the surfaces and the ventilation air.

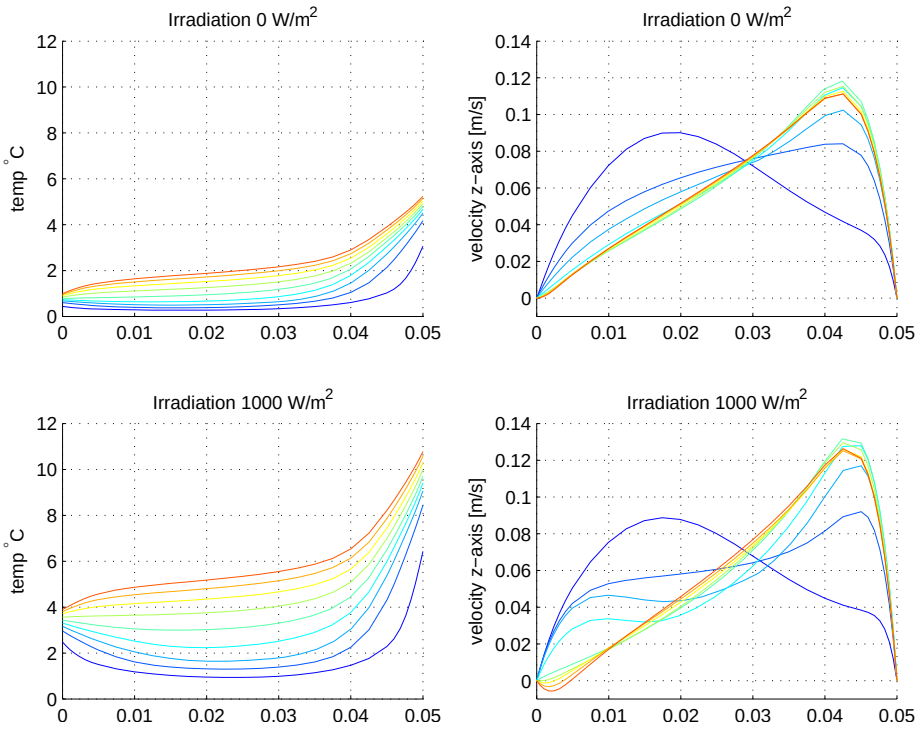

FIGURE 4.4: *Temperature and velocity profiles for cases with 0 and 1000 w/m^2 irradiation and a 3 l/s ventilation flow.*

Attentive readers might note a difference between the case of 500 W/m^2 irradiation and a flow of 3 l/s, presented in figure 4.1 on page 39 and in figure 4.3 on the previous page. This is because the calculated absorbed irradiation in the inside pane is mistakenly set to only 8% for the flow variation parameter study and to 10% for the irradiation parameter study. This was discovered late in the analysis and is judged not to influence the analysis. The method for applying absorption of solar irradiation is already a simplification and it is in any case the resulting surface temperatures that are used in the analysis. The irradiation is just a convenient way of rising the surface temperatures, without using isothermal surfaces.

4.2.3 Dependency on Cavity Depth

The convective heat flux for both surfaces decreases as the depth is enlarged, which results in a almost constant preheating of the ventilation air.

The dependency on the depth of the cavity is in opposition to the predictions of the ISO standard.

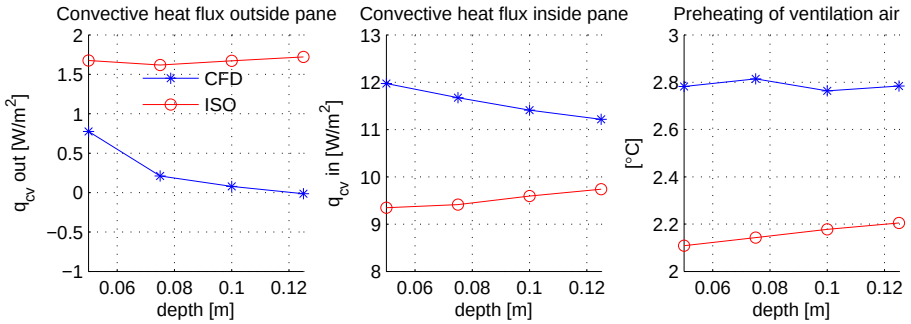

FIGURE 4.5: *Dependency on cavity depth. Comparison of main results from CFD simulations with solar irradiation and corresponding ISO standard calculations*

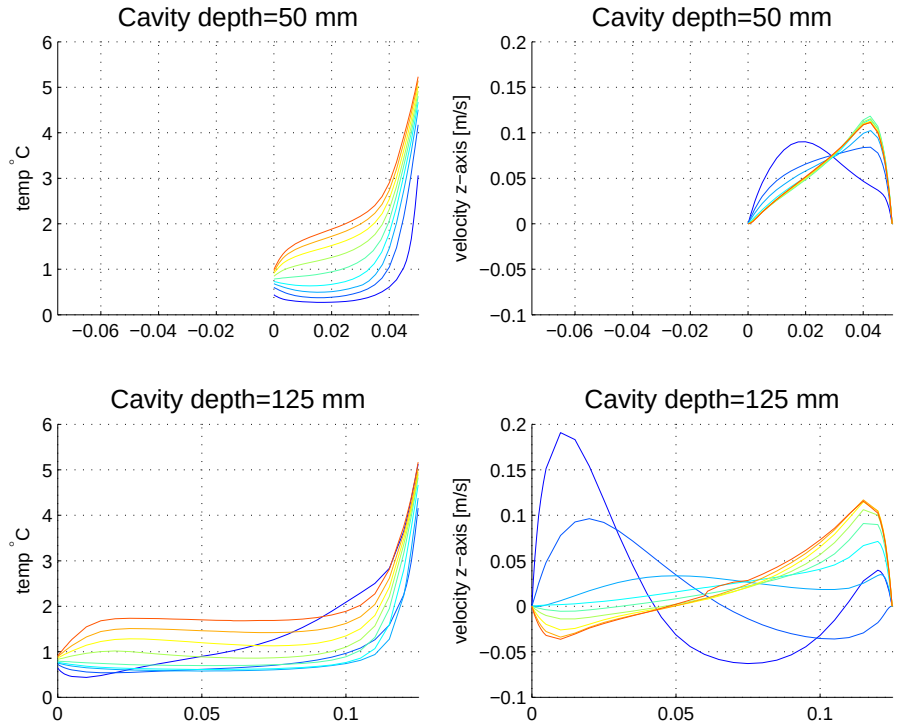

FIGURE 4.6: *Temperature and velocity profiles for cases with cavity depth of 50 and 125 mm for 3 l/s ventilation flow.*

By increasing the depth of the cavity the average velocity of the forced flow is lowered. It is surprising that the lowered average velocity and the consequently longer time the air takes to flow through the cavity does not result in a increased preheating of the air. But looking at temperature and

velocity profiles for depth of 50 and 125 mm, plotted in figure 4.6 on the preceding page, it is noticeably that the temperature increase of the air is confined to an area close to the warm surface of roughly the same size for the two depths. As expected does natural buoyancy becomes more dominating as the depth is increased and the velocity of the forced flow is lowered. But the resulting velocities in the areas close to the warm surface are of almost equal magnitude independent of the cavity depth.

4.2.4 Dependency on Window Height

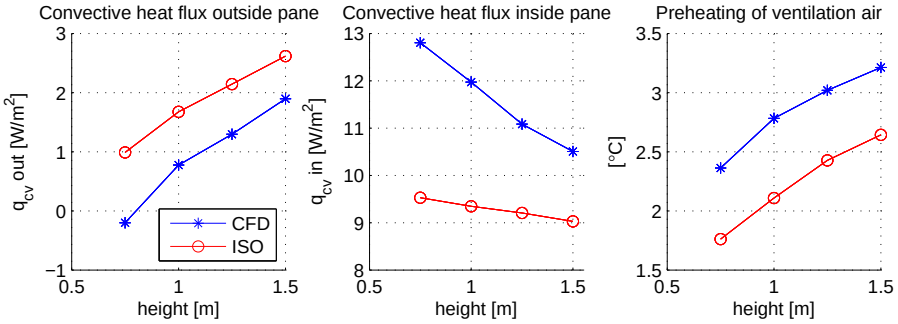

FIGURE 4.7: *Dependency on window depth. Comparison of main results from CFD simulations with solar irradiation and corresponding ISO standard calculations*

The higher the window the more time it takes for the ventilation to air pass through the cavity and the more it is heated. The air temperature in the cavity increases with the height as can be seen i figure 4.8. Therefore the higher the window the higher the temperatures are at the top of cavity and this leads to a larger convective heat flux to the cold outer pane and lower to the warm inner pane. By increasing the height of the window a higher preheating is therefore achieved. But at the same time the convective flux (per square meter) from the inside surface to the cavity is decreased. For the outside surface the convective heat flux increases both nominal and per square meter with increased height.

4.3 Conclusion

Increasing the ventilation rate lowers the overall temperature of the air in the cavity, including the preheating. This increases the convective flux from the warm inner surface and decrease the flux to the cold outer surface. For flows larger than 4 l/s does the heat flux to the outside surface even become negative. The pane is heated by radiation from the inner pane causing the

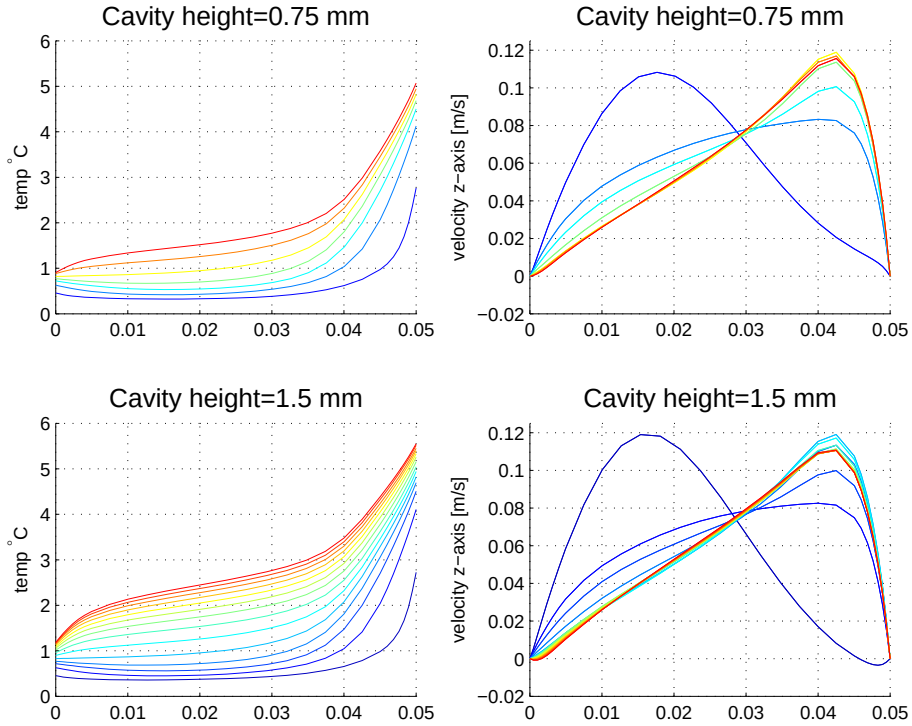

FIGURE 4.8: *Temperature and velocity profiles for cases with window height of 0.75 and 1.5 m and 3 l/s ventilation flow.*

pane to have a higher temperature than the air in the cavity and the direction of the convective heat flux is reversed.

Variation of the solar irradiation absorbed in the panes has shown a linear relationship between the convective heat fluxes and the amount of solar irradiation.

The convective heat fluxes through both surfaces decreases with increased cavity depth. And an almost constant preheating of the ventilation air was found. At least for the range investigated does an increase of the cavity depth improve the effect of the ventilated cavity.

Increasing the window height causes an improved preheating of the ventilation air, but at the expense of increased heat loss through the outer pane.

The parameter variations have generally shown that the ISO standard rather poorly predicts the convective heat fluxes in the cavity. In the next chapter the predictions of the convective heat fluxes will be analyzed in more detail.

Chapter 5

Analysis of CFD Simulation Results

The ISO standard is generally rather poor at predicting the convective heat fluxes in ventilated cavities. Especially for high ventilation flows does the ISO standard method produce large errors.

The errors of the ISO standard can at least partly be explained by the underlying assumption, that the volume average air temperature represents the air temperature for calculations of convective heat fluxes. The convective heat flux, q_{cv} is calculated from the convective heat transfer coefficient, h_{cv} and the temperature difference between the surface and the air.

$$q_{cv} = h_{cv} \left(T_{surface} - T_{air} \right) \tag{5.1}$$

The convective heat transfer coefficient, h_c is essentially a function of the flow characteristics of the near surface flow and is a measure for the heat resistance of the boundary layer.

For natural convection in a closed domain, like the unventilated cavity, the air temperature is commonly represented by the average temperature of the whole volume, T_{avg}. Which works excellent because T_{avg} by definition is located somewhere in the middle of the surface temperatures.

But the for ventilated cavities the temperature profiles show that the temperature increase of the air is confined to an area close to the warm inner side. The average air temperature is much higher than the temperature of the air halfway between the surfaces. For many of the simulated cases, the lowest air temperature is actually found close to halfway between the surfaces. Since the average temperature is higher than the surface temperature of the outer pane, it is a bad choice for capturing negative heat flux from the outer pane.

Another method of representing the air temperature is the mean temperature, T_m. The mean temperature is commonly used for forced internal flows,

because it represents the advective heat flux. In order to represent the advective flux the mean temperature can only represents a plane (cross section) in the flow and not a volume.
The advective heat flux is defined as:

$$Q_{adv} = \int_A \rho c_p u T dA \tag{5.2}$$

If a mean temperature is defined such that it can represent the adcevtive heat flux Q_{adv}

$$Q_{adv} = \int_A \rho c_p u dA \cdot T_m \tag{5.3}$$

The mean temperature is then defined as:

$$T_m = \frac{\int_A \rho u c_p T dA}{\int_A \rho c_p u dA} \tag{5.4}$$

Where:

A is the area of the cross section $[m^2]$

It is possible to calculated T_m for the CFD simulations by using the temperature and velocity profiles. But while the mean temperature efficiently represent the advective heat flux, it can not meaningfully be used to calculate the convective heat flux transverse to the flow. Especially for the low to moderate ventilation flows high temperatures and high velocities coincide, which makes the mean temperature higher that the average temperature.

Neither of the commonly used representations of the air temperature is apparently useful for predicting the convective heat flows in a ventilated cavity with asymmetrical heated surfaces. This leaves us with two options. First option: To use an arbitrary air temperature that can represent the temperature midway between the surfaces. But the very asymmetrical temperature profiles make it quite difficult to represent the air temperature of the cavity by a single temperature node. Second option: Not to use a single air temperature.

The first option is explored in section 5.1 on the next page, by modifying the ISO standard method. The other option, not to use a single air temperature, can quickly lead to a 'coarse' CFD simulation. Because as soon as multiple air temperature nodes are implemented, it raises a need to calculated the energy flow between the nodes. When complex flows, e.g. natural buoyancy, are involved there is soon a need to know not only the temperature of the node but also the flow, to be able to calculate convective and advective heat fluxes.

Another way of escaping the need for at single air temperature node is to look at the development of temperature profiles up through the cavity as a one dimensional transient heat flux. The time is then linked to the vertical position in the cavity. This method is explored in section 5.2 on page 53.

5.1 Modification of the ISO Standard Method

The ISO standard continuously underestimates the convective heat fluxes and it therefore seems likely at fist glance, that the ISO standard underestimates the convective heat transfer coefficients. But there is a coupling between the average air temperature and the convective heat transfer coefficients. By increasing the heat transfer coefficients the average air temperature becomes closer to the average surface temperature. This can be shown by combining equation (2.25) and (2.26) chapter 2.2.3 on page 17 and separate the convective heat transfer coefficients for the two surfaces, $h_{cv,in}$ and $h_{cv,out}$ we get:

$$T_{gap} = T_{av,surfaces} - \frac{\rho \cdot c_p \cdot d}{H(h_{cv,in} + h_{cv,out})} \cdot V(T_{cav,out} - T_{cav,in}) \qquad (5.5)$$

By increasing $(h_{cv,in} + h_{cv,out})$ the average air temperature, T_{gap} becomes closer to the average surface temperature, $T_{av,surfaces}$. It follows that a higher T_{gap} makes it even more impossible to capture the large negative heat flux observed in the CFD simulations.

It is the problem of representing the air temperature distribution by one average. For fully developed internal flows the average temperature method appears to works excellent and gives reliable results in many different applications. But for flows dominated by natural buoyancy and/or in thermal entry region the average temperature does not necessarily represents the bulk of the air, as the temperature profiles from the CFD simulations show.

To improve the method presented by the ISO standard it is consequently necessary to decouple the air temperature and the heat transfer coefficients, and introduce an arbitrary or bulk air temperature. But it is still necessary to have some kind of connection between the surface heat fluxes and the bulk temperature. It is not possible to use a predefined temperature like e.g. the inlet temperature. Because a fixed predefined temperature will not be able to capture the shift in the direction of the convective heat flux for increased ventilation rate, observed in the CFD simulations.

So there still is a need for some kind of coupling between air temperature and the heat transfers. A simple solution is to let air temperature depend only on one of the heat transfer coefficients. Since the convective heat flux is much

larger for the inner surface it seems reasonable to couple inside convective heat transfer coefficient and air temperature.

The CFD simulations have revealed that the flow patterns are not symmetrical. So there is no obvious reason why the convective heat transfer coefficients should be identical for both surfaces. Perhaps it is possible to obtain better results by adjusting the influence of the forced ventilation on the convective heat transfer coefficients. But to maintain some connections with reality we must impose that the convective heat transfer can not be less that the conductive heat transfer for stationary air. This also excludes negative heat transfer coefficients.

By implementing a optimization algorithm with an adjusting of convective heat transfer coefficients as variables, it is possible to it quickly investigate whether it seems likely that the ISO standard method can be improved by not using average temperature. The dependency on ventilation rate and solar irradiation seems to be the most complex. The optimization algorithm is therefore applied on a parameter variation of flow rate with none and 500 W/m^2 solar irradiation. The algorithm finds the best fit between the heat fluxes found by the CFD simulations and the modified ISO standard method with the variables a_1 and a_2 as presented in equation (5.6)-(5.7).
Variables for the convective heat transfer coefficients:

$$h_{cv,in} = 2h_c + a_1 \cdot V \tag{5.6}$$

$$h_{cv,out} = 2h_c + a_2 \cdot V \tag{5.7}$$

The air temperature T_{gap} is only coupled to the inside heat transfer coefficient:

$$T_{gap} = T_{av,surfaces} - \frac{\rho \cdot c_p \cdot d}{H \cdot h_{cv,in}} \cdot V(T_{cav,out} - T_{cav,in}) \tag{5.8}$$

Where:

h_c is the convective heat transfer coefficient for non-ventilated cavities given by equation (2.14) page 15 $[W/m^2K]$.

a are the variables for adjusting the convective heat transfer coefficient.

The results of the optimizations are plotted in figure 5.1 on the facing page. The adjustment of the velocity component of the warm inside, a_2, appears close to linear and quite similar for the two cases with and without solar irradiation. A linear relationship means that the convective heat transfer coefficient is a second order function of the average velocity, $h_{cv,in} = h_c + (aV^2 + bV + c)$.

But not so for a_1, the component for the cold outside. For both cases there appears to be a initial drop of a_1 and after a turning point it rises again. But the

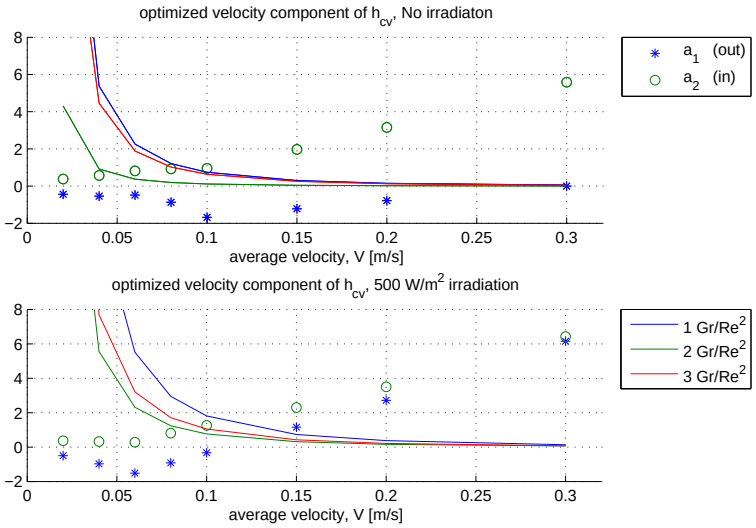

FIGURE 5.1: *Results of the optimization of the velocity component for the heat transfer coefficients plotted together with possible calculations of* $\frac{Gr}{Re^2}$.

turning points are located different, and a_1 rises to a much higher magnitude for case with solar irradiation than for case without.

To investigate whether the optimized velocity component could be linked to the flow pattern the results are plotted together with possible calculations of $\frac{Gr}{Re^2}$. Where Gr is the dimensionless Grashof number and Re is the dimensionless Reynolds number. This term is normally used to determine if the natural convection or the forced flow can be assumed negligible [22] [23]. For $\frac{Gr}{Re^2} \ll 1$ the natural convection can be assumed negligible and for $\frac{Gr}{Re^2} \gg 1$ the forced flow can be assumed negligible.

$$\text{Grashof} \qquad Gr = \frac{g\beta(T_s - T_\infty)L^3}{\nu^2} \qquad \text{Ration of buoyancy to viscous forces} \tag{5.9}$$

$$\text{Reynolds} \qquad Re = \frac{VL}{\nu} \qquad \text{Ratio of inertia to viscous forces} \tag{5.10}$$

and

$$\frac{Gr}{Re^2} = \frac{g\beta(T_s - T_\infty L^2)}{V^2} \tag{5.11}$$

Where

T_s is surface temperature, $[K]$

T_∞ is the air temperature at free stream conditions, $[K]$

L is the characteristic length. In this case L is the distance between the panes (cavity depth), $[m]$.

ν is the viscosity, $[kg/s \cdot m]$

The tree different calculations of $\frac{Gr}{Re^2}$ are for

1. $\frac{Gr}{Re^2}$ is for the surface temperature equal the inner pane surface temperature $T_s = T_{in}$.

2. $\frac{Gr}{Re^2}$ is for the surface temperature equal the outer pane surface temperature $T_s = T_{out}$.

3. $\frac{Gr}{Re^2}$ is for the surface temperature equal the average pane surface temperature $T_s = (T_{out} + T_{in})/2$.

The free stream air temperature, T_∞ is in all cases set to inlet temperature. As can be seen from figure 5.1 on the previous page, there is no obvious relationship between $\frac{Gr}{Re^2}$ and the optimized heat transfer coefficients. But if compared to the flow profiles, appendix A on page I, there is actually quite good correlation between $\frac{Gr}{Re^2} > 2$ and the flow patterns. Especially for 2. $\frac{Gr}{Re^2}$ (outside pane surface temperature).

5.1.1 ISO Standard Method Conclusion

The fundamental flaw in the ISO standard is representing the temperature node of the cavity by the volume average temperature. But it doesn't appear possible to improve the method implemented in the ISO standard by decoupling the convective heat transfer coefficients and the cavity air temperature. This does introduces an arbitrary air temperature instead of the average air temperature. But this does not solve the problem of correct convective heat transfer. It might be possible to find some experience based function for the heat transfer coefficients. But no obvious correlations have been found. It is therefore chosen to stop developing on the foundation of the ISO standard method for ventilated cavity, and instead approach the ventilated cavity from a very different direction.

5.2 Transient Analysis of Temperature Development

A completely different solution to the problem of representing the cavity temperature could be to look at it as a transient heat flux problem. The development of the temperature profiles up through the cavity has similarities to 1-dimensional transient heat flux temperature development. Looking at the temperature profiles in figure 5.2, they could easily be mistaken for time dependent temperature profiles for a wall suddenly exposed to asymmetrical heating on the two sides. Instead of representing a specific height in the cavity, the profiles could equally represent a specific time duration.

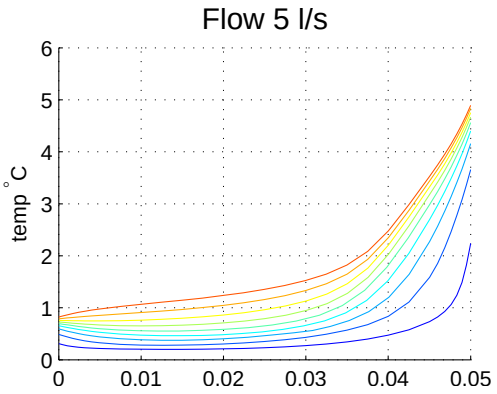

FIGURE 5.2: *Temperature profiles for case with 5 l/s flow and no solar irradiation.*

Looking at the heat fluxes in the cavity as a transient problem naturally presumes a time dependency, but the cavity is at steady state equilibrium. This apparent contradiction can be solved by looking at the time dependency, not for the system as a whole, but for the ventilation air as it moves upwards in the cavity. It then follows that for $t_0 = 0$ the air enters the cavity and exits at $t_{end} = \frac{V}{H}$. Where V is the average velocity and H is the height of the cavity.

If the convective heat flux through the surfaces can be effectively simulated by looking at it as a transient problem, the preheating of the ventilation air can easily be calculated, because of the conservation of energy. The whole system is considered a steady state system and as such must have conservation of energy. The difference between the energy entering and leaving the cavity through the surfaces is therefore the heating of the ventilation air.

$$Q_{in} = Q_{out} + Q_{adv} \tag{5.12}$$

which gives:

$$\Delta T = \frac{Q_{out} - Q_{in}}{\rho c_p \varphi} \tag{5.13}$$

Looking at the convective heat flux as a transient problem make it possible to capture the negative heat flux from the outer pane, because it can explain why the lowest air temperatures in many cases are located somewhere in the middle of the cavity. Approaching the heat flux transverse to the main flow direction as a transient one-dimensional problem is of course a gross simplification and raises some other problems.

The first problem is that the apparent thermal conductivity of fluid in motion is not homogeneous, because it depends on the local Nusselt number that depends on the derivative of the velocity and the amount of turbulence, if any. If it is assumed that the flow is laminar and only in the vertical direction, then the Nusselt number only depends on the derivative of the velocity.

$$\lambda = \lambda_{air} Nu \tag{5.14}$$

Where Nu is a function of the derivative of the velocity, V and coordinate, x.

$$Nu = f\left(\frac{\partial V}{\partial x}\right) \tag{5.15}$$

The apparent thermal capacity is not necessarily constant either. Because of the differences in velocity, the thermal capacity not only depends on thermal capacity of the fluid, but also the mass flow, or more accurate on the relative mass flow (velocity). If the time is linked to the average velocity of the forced flow, then the transient temperature profile develops up trough the cavity with the speed of the average velocity. But for sections with a relatively higher velocity the mass flow is higher and therefore the mass that needs to be heated is larger than the average.

$$c_p = \frac{c_p u}{u_{avg}} \quad [J/kgK] \tag{5.16}$$

This would imply negative thermal capacities for sections with negative velocities. But applying the above assumption, that the flow is only in the vertical direction and that therefore no transverse flow exist, no negative velocities can exist either. Negative velocities require a swirling motion, and therefore transverse flow, to keep the mass balance.

The assumption of flow only in vertical direction can in some degree cover the flows dominated by forced flow, but is far fetched for flows dominated by natural buoyancy.

5.2.0.1 Simple Assumptions for Material Parameters for Transient Calculations.

But before trying to determine the flow pattern and how to deal with the assumptions of laminar and unidirectional flow, let us use some simpler assumptions. The simplest assumption of the material parameters of the air is a uniform thermal capacity and Nusselt number. The thermal capacity is simply set to that of air. The Nusselt number is calculated by the ISO standard method. But since it is expected that the heat transfer coefficients differ between the two surfaces simple variations of the Nusselt number is also implemented.

$$Nu = Nu_n + Nu_f \tag{5.17}$$

Where NU_n is the Nusselt number resulting from the natural buoyancy and Nu_f is the Nusselt number resulting from the forced ventilation.
From the ISO standard method we have:

$$h_{cv} = Nu_n \frac{\lambda}{d} + 4V \tag{5.18}$$

The general definition of convective heat transfer coefficients is $h_c = Nu\frac{\lambda}{d}$ and we can therefore rewrite as:

$$Nu = h_{cv}\frac{d}{\lambda} = Nu_n + \frac{4Vd}{\lambda} \tag{5.19}$$

The Nusselt number derived from the forced ventilation flow is hence $Nu_f = \frac{4Vd}{\lambda}$.

$$\text{Nu ISO:} \qquad Nu = Nu_n + Nu_f \tag{5.20}$$

Natural and forced flows can not only assist but also oppose each other. To take this into account the Nusselt numbers are respectively added or subtracted for assisting or opposing flows. The ISO standard implicitly suggests a linear relation between the natural and forced Nussselt number.

$$\text{Nu 1:} \qquad Nu = Nu_n \pm Nu_f \tag{5.21}$$

But [22] suggest the following expression to combine the forced and convective Nusselt number in relation to whether the flows oppose or assist each other.

$$\text{Nu 2:} \qquad Nu^3 = Nu_n^3 \pm Nu_f^3 \tag{5.22}$$

For the cases with different Nusselt numbers for each side, the resultant Nu are simply applied for each half of the cavity.

5.2.0.2 Boundary Conditions for Transient Calculations.

According to the temperature profiles the surface temperature of the outer surface is rather stable. It does not change much over the height of the window. Therefore it is a reasonable assumption to have a fixed surface temperature for this side.

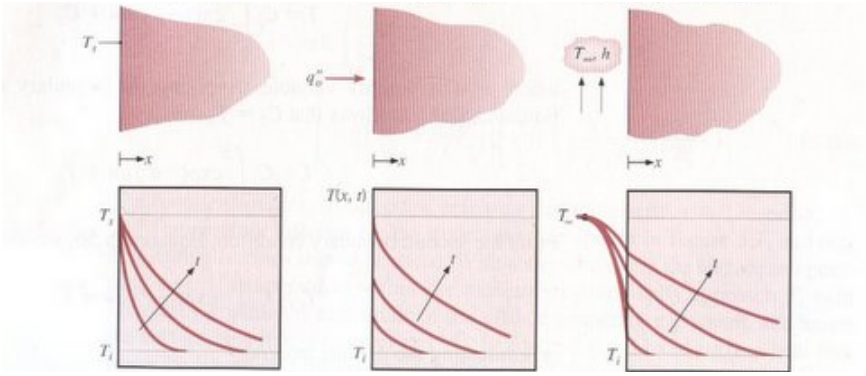

FIGURE 5.3: *Transient temperature development for three surface conditions: constant surface temperature, constant heat flux and surface convection. Reproduced from [22].*

The surface temperature of the inner surface varies over a larger range and increases with the height of the window. The temperature development near the inner pane appears to be better represented by boundary conditions associated with a fixed ambient air temperature and a surface heat transfer resistance. As for the CFD simulations the surface heat transfer resistance is set to 1.72 $[m^2K/W]$, which included a double pane window and internal surface heat resistance. But since radiation between the two panes are included in the CFD simulations, it is also necessary to take this radiative heat flux into account as well as any solar irradiation.
The radiative heat flux is calculated as:

$$q_{rad} = \sigma_s \varepsilon (T_{out}^4 - T_{in}^4) \tag{5.23}$$

where

σ_s is Stefan-Boltzmann constant $\sigma_s = 5.67 \cdot 10^{-8}$ $[W/m^2K^4]$

ε is combined emissivity [-]

For the transient calculations a numerical one-dimensional implicit method, that meets these specific requirements, has been developed.

5.2.1 Results of Transient Method

The results of the transient calculations are plotted in figure 5.4. The transient calculations all have a significant better prediction of the convective heat fluxes through the inner surface over the whole range of ventilation rates.

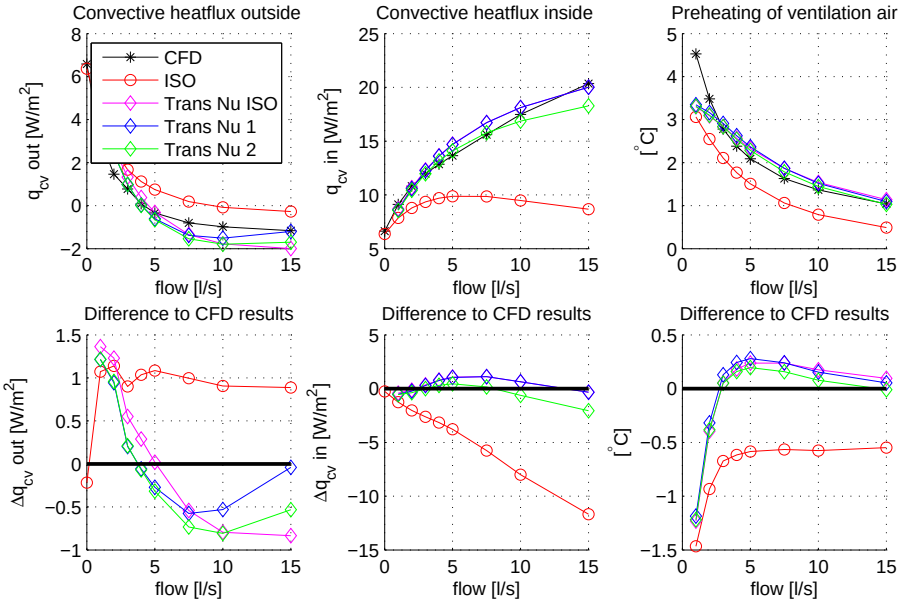

FIGURE 5.4: *Variation of ventilation rate. Top: Comparison of convective heat flux calculated with ISO standard and transient calculations. Bottom: Difference between the CFD results and the different calculations.*

For the outside heat fluxes the transient calculations generally have better predictions than the ISO standard. The transient calculation of Nusselt numbers reflecting if flows are opposed has a better prediction for extremes with either low or high ventilation rates. But for the very low ventilation rates of 1 and 2 $[l/s]$ the predictions are in the same range as the ISO standard. The very low ventilation rates are of course more dominated by natural convection and therefore furthest from the assumptions behind the transient calculations.

Considering the simplifications of the material parameters for the transient calculations, they show remarkably good results. It seems like Nu 1 has the best predictions. Nu 1 has a linear relationship between natural and forced Nusselt numbers and taken into account whether the flows are assisting or opposing.

The transient predictions of the variations of cavity depth is plotted in figure 5.5 on the next page. The transient method produces better results than the ISO standard method. But it is not as convincing as seen for the variation of ventilation rate. The larger the depth of the cavity, the more the flow pattern

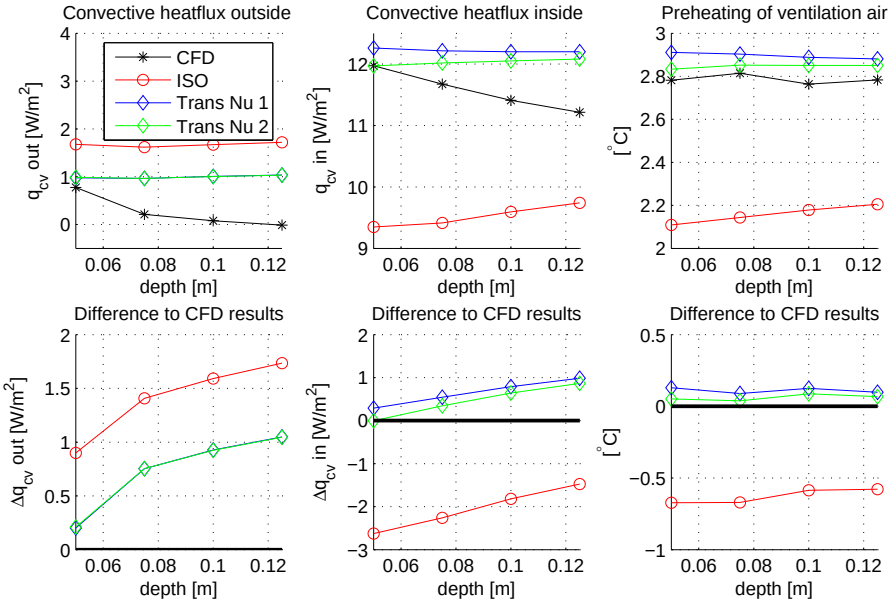

FIGURE 5.5: *Variation of cavity depth. Top: Comparison of convective heat flux calculated with ISO standard and transient calculations. Bottom: Difference between the CFD results and the different calculations.*

is dominated by natural convection. As noted earlier the transient method is not very efficient for flows dominated by natural convection.

The results of the transient calculations have almost no variation with the depth. This is even though the average velocity and hence the time span varies with more than a factor of two. But Nu varies close to linearly with the depth of the cavity. This means that when the depth and hence the time span is doubled the thermal resistance is also doubled. The transient method is therefore not able to predict the positive effects of increasing the depth of the cavity.

For the variations of solar irradiation/surface temperatures the transient predictions has a continuously very good fit with the convective heat flux through the inner surface. It is not quite so good for the outer surface, but still much better than the ISO standard. Just like the CFD simulations the transient calculations show a linear relationship between the irradiation and the heat fluxes. As for the other parameter variations the error of the transient calculation appears to grow as the flow pattern becomes increasingly dominated by natural convection.

The transient results for the parameter variation of ventilation rate with increased solar radiation is plotted in figure 5.7 on the facing page. The results are not as close as for the other parameter variations. But it is still a significant

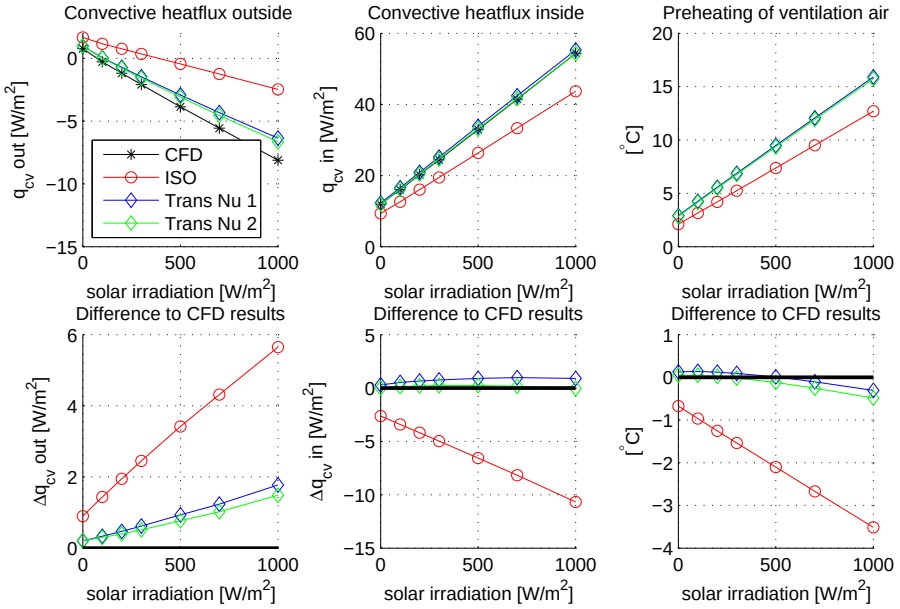

FIGURE 5.6: *Variation of solar irradiation. Top: Comparison of convective heat flux calculated with ISO standard and transient calculations. Bottom: Difference between the CFD results and the different calculations.*

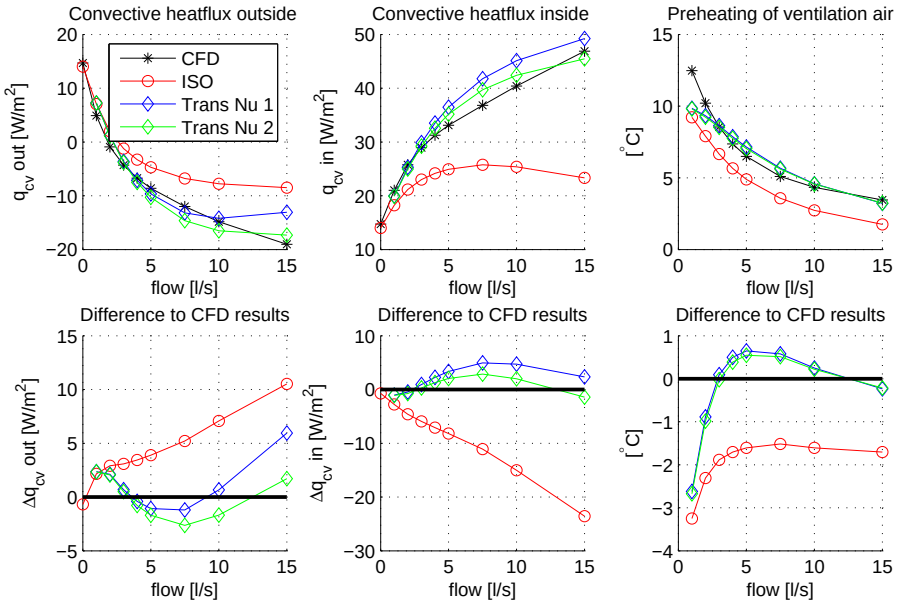

FIGURE 5.7: *Variation of ventilation rate with 500 W/m^2 solar irradiation. Top: Comparison of convective heat flux calculated with ISO standard and transient calculations. Bottom: Difference between the CFD results and the different calculations.*

improvement of the ISO standard method.

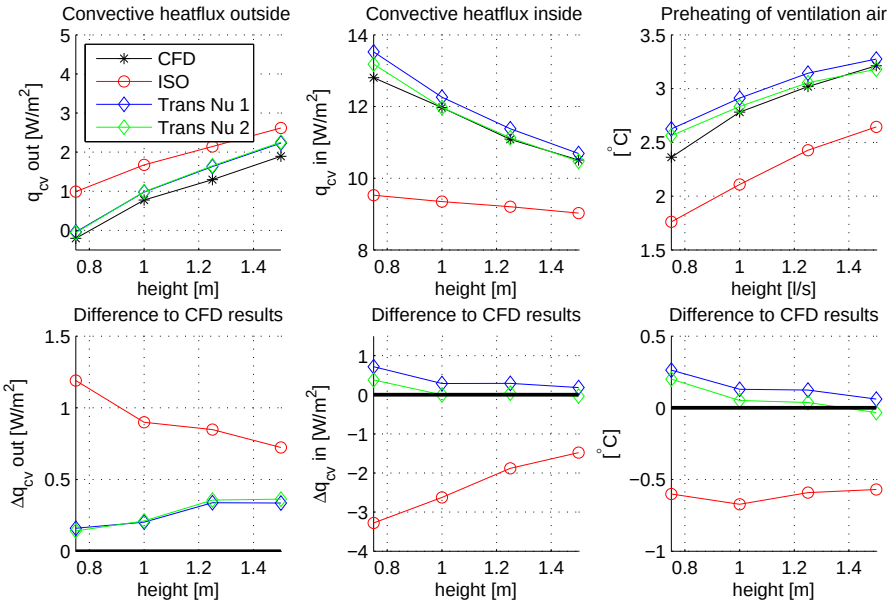

FIGURE 5.8: *Variation of window height. Top: Comparison of convective heat flux calculated with ISO standard and transient calculations. Bottom: Difference between the CFD results and the different calculations.*

5.3 Implementation of Transient Method in WinVent Program

The CFD simulations in the earlier chapters have focused specifically on convective heat fluxes in cavity. Now focus is changes to the whole window – at least the whole vision area.

Air flow windows cover a wide range of configurations of panes and cavities ventilated or not. But the obvious choice and the configuration examined in the project is a 1+2 solution – one single pane on the outside of the ventilated cavity and a double pane on the inside – with the ventilation air moving upwards in the cavity. The purpose of the single pane on the outside is only to separate the ventilated cavity from outside environment. The insulation of the outside pane has no real value. But the double pane on the inside ensures that the surface temperature on the inside of the window is high enough not to cause any risk of condensation. The ventilation air has to move upwards in the cavity in order to benefit from the natural buoyancy flow pattern. Sideways or downwards flow will cause a much lower preheating of the ventilation

air. Other configurations of the air flow window might also produce desired thermal effects. But considering the time frame and the projects focus on developing a new calculation method it is chosen only to investigate the 1+2 solution.

It is presented how the governing equations given by the ISO standard method for the heat fluxes in windows presented in chapter 2, are implemented in the Matlab program called WinVent. For the ventilated cavity both the ISO standard method and the transient method developed in chapter 5.2 are implemented. This makes it possible to evaluate the impact of the improved method. There are commercial programs on the market, which have implemented the ISO standard and can make very detailed calculations. Especially the WIS program by Windat is widely accepted as the reference for window calculations. But by developing WinVent it is possible to change fundamental equations, like the method for the ventilated cavity.

5.3.1 Equilibrium Equations

The heat fluxes are found by setting up equilibrium equations for each temperature node and solving the resulting nonlinear system of equations, with the temperatures as the unknowns.

The thermal resistances of the panes are so small, that they count for less than 1% of the total resistance. To ease the program buildup and decrease the computational time, the thermal resistances of the panes are omitted. This leaves only 3 temperature nodes, one for each pane, and therefore only 3 unknown variables to be found.

The non linear equations system consist of equilibrium heat flow equations for the 3 temperature nodes. For each pane the radiative, Q_{rad} and convective, Q_{cv} or Q_c, heat fluxes together with the absorbed solar irradiation have to be in equilibrium. The calculations of the heat fluxes are explained in detail in chapter 2.

$$\text{Node pane 1:} \quad 0 = Q_{rad,out} + Q_{c,out} - S_1 - Q_{cv,b,1} - Q_{rad,1} \tag{5.24}$$

$$\text{Node pane 2:} \quad 0 = Q_{rad,1} + Q_{cv,f,2} - S_2 - Q_{c,2} - Q_{rad,2} \tag{5.25}$$

$$\text{Node pane 3:} \quad 0 = Q_{rad,2} + Q_{c,3} - S_3 - Q_{c,in} - Q_{rad,in} \tag{5.26}$$

The only difference between the ISO standard method and the transient method for the cavity is the calculation of the convective heat fluxes in the ventilated cavity, $Q_{cv,b,1}$ and $Q_{cv,f,2}$

5.3.1.1 ISO Standard Method for Ventilated Cavity

When calculating the heat balance for the ventilated cavity the thermophysical properties of the air is needed in calculation of the characteristic height H_0 and such the average air temperature, T_{cav}. A simple iteration procedure is implemented using the surface average temperature as initial guess. The resulting air temperature is then used as the next guess until the difference between the input and output cavity temperature is less than $|T_{guess} - T_{cav}| < 0.05$.

The temperatures of the air in the cavity and subsequent the ventilation heat flows, Q_{adv} and Q_{vent} are solved analytically as a function of the surface temperatures.

5.3.1.2 Transient Method for Ventilated Cavity

As explained in chapter 5.2, the time dependency in the transient method linked is to the height of the window. The (for the whole window) steady state convective heat fluxes are found by integration over the time/height.

The transient method is solved with a one-dimensional implicit finite difference method, using control volumes. See for example [24]. The boundary condition for the outside surface of the cavity is a constant temperature. The inside surface boundary condition is somewhat more complicated, because of the need to achieve the height (time) dependent surface temperature increase. The boundary condition is therefore achieved by applying the heat flow balance to the surface.

$$\text{Boundary condition:} \quad 0 = Q_{rad,1} + Q_{cv,f,2} - S_2 - Q_{c,2} - Q_{rad,2} \quad (5.27)$$

There is no heat capacity attached to the node because it is a surface node. For each timestep the heat fluxes constituting equation, (5.27) is calculated as a functions of the surface temperature. The radiative heat fluxes are calculated by use of equation (2.30).

$$Q_{rad,i} = A \cdot (J_{f,i} - J_{b,i-1})$$

The convective heat flux from pane 3, $Q_{c,2}$ is calculated by use of equation (2.10).

$$Q_{c,2} = h_{c,2} A (T_{f,3} - T_{b,2})$$

The convective heat transfer coefficient, $h_{c,2}$ is kept constant though, and calculated from the average/steady state surface temperature of pane two. The convective heat flux from the surface into the cavity, $Q_{cv,f,2}$ is inherent to the transient calculation.

The boundary condition for the inside surface of the cavity has the peculiar consequence, that the surface temperature of pane two is actually not used in calculating the convective heat flux from this surface to the cavity.

The material properties of the air are based on the simple assumptions presented in chapter 5.2.0.1. The thermal conductivity is based on $Nu\ 2$, the third degree relationship of the Nusselt numbers for forced and natural convection, equation (5.22). The third degree relationship appears to have the best overall fit.

The transient method is implemented with a uniformly spaced grid of 26 control volumes and a timestep of $0.05\ s$, comfortably below the critical timestep for a likewise but explicit implementation. This ensures sufficient low numerical errors.

5.3.2 Impact of Transient Method vs. ISO Standard Method

The transient method is, as shown in chapter 5.2.1, a significant improvement of the ISO standard method, in terms of prediction of the convective heat flows in ventilated cavity. But they are only a small part of the total heat fluxes in the window and it is important to know whether the method for the ventilated cavity has any impact on the total performance of the window. The impact of the method on the overall performance of windows is therefore evaluated on three different window configurations. Case 1: has a cavity depth of 50 mm and a flow of 3 l/s per meter window width. Case 2 has increased depth of 100 mm and flow of 5 l/s. Case 3 has increased depth of 100 mm and flow of 10 l/s. All three cases are for a solar irradiation of 500 $[W/m^2]$. The results are shown i table 5.1.

Method	parameter	case 1	case 2	case 3
Transient	$U_{eff}\ [W/m^2K]$	0.69	0.55	0.41
	Preheating $[^\circ C]$	10.2	8.4	5.6
	g-value [-]	0.62	0.63	0.65
ISO standard	$U_{eff}\ [W/m^2K]$	0.76	0.69	0.61
	Preheating $[^\circ C]$	8.5	6.5	4.0
	g-value [-]	0.61	0.62	0.63
Improvement	$U_{eff}\ [W/m^2K]$	9%	25%	33%
	Preheating $[^\circ C]$	20%	29%	40%
	g-value [-]	2%	2%	3%

TABLE 5.1: *Comparison of windows thermal performance for transient or ISO standard method for ventilated cavity*

The improvement is defined as:

U_{eff}: $$improvement = \frac{U_{eff,ISO} - U_{eff,tra}}{U_{eff,ISO}} \quad (5.28)$$

preheating: $$improvement = \frac{\Delta T_{tra} - \Delta T_{ISO}}{\Delta T_{ISO}} \quad (5.29)$$

g-value: $$improvement = \frac{g_{tra} - g_{ISO}}{g_{ISO}} \quad (5.30)$$

The transient method has compared to the ISO standard method a large impact on the effective U-value (9 to 33 % reduction) and a on the preheating of the ventilation air (20 to 40 % increase). The impact on the g-value is more modest with an increase of 2 to 3 %.

It would have been appropriate with a comparison to results obtained by CFD simulations. But because of the simplifications of the boundaries, especially the way the absorption of solar irradiation is implemented for the inside surface, makes it impossible to extrapolate to the performance of the whole window.

5.4 Conclusion

The analysis of the ISO standard method has shown that it is necessary to abandon the average air temperature as representation of the cavity air temperature in order to improve the method. It is possible, that by introducing an arbitrary air temperature dependent on only one of the surfaces heat transfer coefficients, predictions by the method can be improved. But the very asymmetrical temperature profiles found in the cavity makes it unlikely that the air temperature can be adequately represented by one temperature node.

The proposed transient method of calculating the heat fluxes has produced remarkably good predictions with very simple calculations of convective heat transfer coefficients. The transient method does have some difficulties predicting the convective heat flux through the outer surface for flows dominated by natural convection. For flow patterns highly dominated by natural buoyancy the assumptions behind the transient method are simply not valid. This results in a overestimation of the heat loss for low ventilation rates, $\varphi < 2 \quad [l/s]$ per meter width of window. The transient method is not able to predict the improved performance of increasing the depth of the cavity either. But the transient method is generally a significant improvement of the ISO standard method.

Implementing the transient method in WinVent has shown that changing the method for the ventilated cavity from the ISO standard to the transient

method has a large impact on the effective U-value (9 to 33 % reduction) and a on the preheating of the ventilation air (20 to 40 % increase). The impact on the g-value is more modest with an increase of 2 to 3 %.

Chapter 6

Thermal Performance of Air Flow Windows

Air flow windows are compared to normal unventilated windows to give a basis for evaluation of the thermal performance. In order to have comparable conditions for the windows performances, they are primarily evaluated for situations with exhaust ventilation.

To acknowledge that normal windows come in a wide range of qualities, the thermal performance characteristics for both a standard and a 'super' version of both double and triple glazed windows are presented. The performance characteristics of the normal windows are calculated with WinVent and checked against the WIS program. Likewise are the glazing properties presented in table 6.1 on the following page imported from the WIS database.

Radiative heat fluxes are reduced by use of low-emissivity coatings on the panes. The coatings can roughly be divided into soft and hard coatings. Soft coatings are the most efficient but are easily scratched and therefore only used in closed cavities, like in normal sealed windows. In a ventilated cavity it is necessary to be able to open up and clean the panes for any dust or particles that may accumulate over time. It is therefore only feasible to use hard coatings.

Both of the normal double pane windows are 4-16-4 configurations with argon gasfilling. For the standard version a clear pane outside and WinDat lowEsoft pane inside are used. For the super version a clear pane is used outside and a iplus SE pane is used inside.

The triple panes are 4-12-4-12-4 configurations with argon gasfillings. A clear pane is used outside and the two other panes are respectively lowEsoft and iplus SE for the standard and the super version

The resulting thermal characteristics are presented in table 6.2 on the next page

name	ir emissivity		solar
	inside [-]	outside [-]	transmittance [-]
iplus SE	0.037	0.837	0.466
WinDat lowEsoft	0.092	0.837	0.666
WinDat hard	0.160	0.890	0.699
WinDat clear	0.837	0.837	0.847

TABLE 6.1: *Main thermal characteristics of different panes including coating. Values are calculated with WIS.*

type		double glazed		triple glazed	
quality		standard	super	standard	super
U-value	$[W/m^2K]$	1.28	1.12	0.82	0.72
g-value	[-]	0.65	0.55	0.56	0.45

TABLE 6.2: *Thermal performance characteristics of normal windows. There are presented both a standard and an optimized 'super' version of double and triple glazed windows.*

The thermal performances of windows are characterized by the heat loss coefficient, U-value, and the solar energy transmittance factor, g-value. The 'dark' heat loss is evaluated for reference winter conditions without solar irradiation. The impact of the solar energy transmittance is evaluated for reference winter conditions including 300 W/m^2 solar irradiation.

As an example of the performance in the heating season are the windows energy balance evaluated for a small apartment (60 m^2) and compared to normal windows with exhaust or balanced ventilation.

6.0.1 Stable g-value

As discussed earlier, the thermal performance characteristics are temperature dependent, because the material properties of the air (or other fill gas) are temperature dependent. In order to achieve simple characteristics is the thermal performance of windows calculated at reference winter boundary conditions, according to the ISO standard – presented in table 2.1 on page 12.

Just for good measure is it controlled whether the g-value is stable, or if it depends on the amount of solar irradiation. The g-values dependency on solar irradiation for three different flow rates are shown in figure 6.1 on the next page. The g-values are not completely stable, but they change so little that they can be assumed stable.

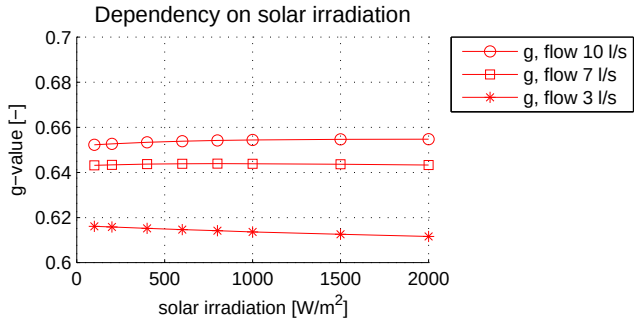

FIGURE 6.1: *G-values dependency on amount of solar irradiation.*

6.0.1.1 Configuration of Air Flow Windows

The thermal performance of air flow windows depends of course on the specific configuration of the window; type and place of low-emissivity coatings, cavity depths etcetera. But it also depends on the specific operational conditions – the ventilation flow rate.

Two different 1+2 configurations of the air flow windows are used in this analysis of thermal performance. 1+2 refers to 1 outside pane and 2 (double) panes on the inside of the cavity. The first configuration is a 'standard' quality air flow window, with a standard double pane, U-value of 1.28 W/m^2K, on the inside of the cavity, and no coatings in the cavity. The second configuration is improved with a hard low-emissivity coating on one side of the cavity.

window		'standard'	'super'
buildup		1+2	1+2
inside db pane U.	$[W/m^2K]$	1.28	1.28
cavity coating		no coating	hard coating
cavity depth	$[mm]$	50	50
window height	$[m]$	1	1

TABLE 6.3: *Configurations of air flow windows for thermal performance analysis.*

6.0.2 Thermal Performance without Solar Irradiation.

The effective U-value depends on the ventilation flow. In figure 6.2 on the following page are plotted the effective U-values for the two configurations of air flow windows as function of the flow rate. To comparison are plotted the U-value of the two normal windows. The thermal performance is evaluated at reference winter conditions.

The normal windows perform better for situations without ventilation, but that is to be expected. The increased depth of the cavity in the ventilation windows improves the convective resistance of the cavity, but that can not compensate for the effects of soft low-emissivity coating and a argon gas filling in the sealed triple glazed windows. But the effective U-values of the air flow windows drop with increased flow, and for flows larger than 3 l/s do even the 'standard' air flow window perform better than the triple glazed 'super' window. The super version of the air flow window reaches effective U-values below $0.2\ W/m^2K$ for flows larger 6 l/s

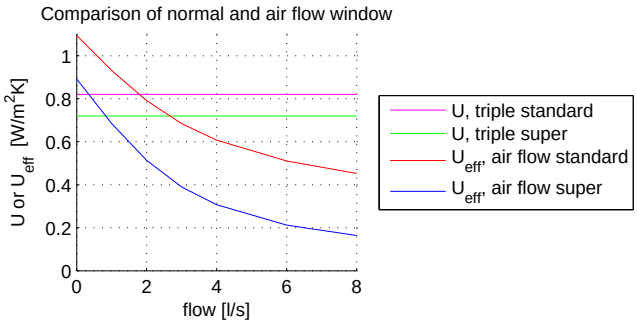

FIGURE 6.2: *Comparison of the effective U-value (U_{eff}) and U-value for normal windows, for different ventilation flows.*

The ventilation heat loss is a significant part of the total heat loss. To show the impact on the total heat loss, including ventilation loss, it is plotted in figure 6.3.

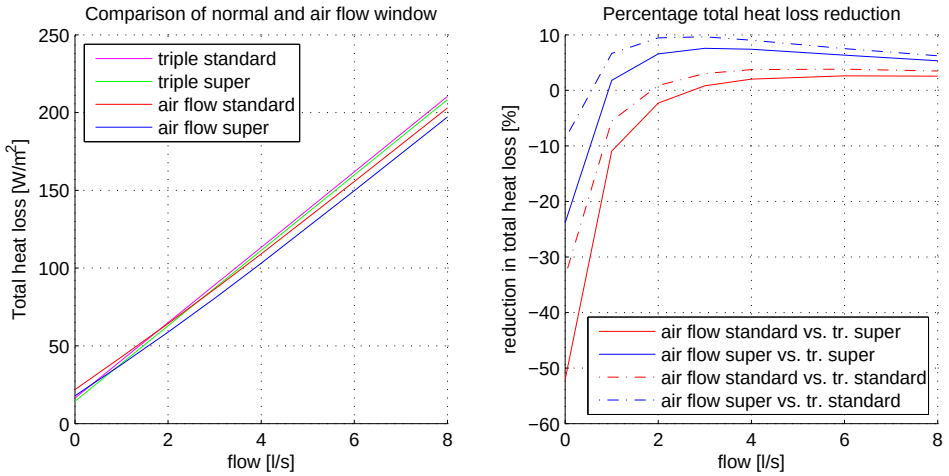

FIGURE 6.3: *Left: The total heat loss, including ventilation loss.*
Right: Total Percentage reduction in total heat loss compared to triple glazed 'standard' and 'super'.

To the right in the figure are plotted the percentage reduction in total heat loss compared to the normal triple glazed windows. The percentage reductions are calculated by:

$$reduction = 100\% \cdot \frac{(Q_{tot,n} - Q_{tot,a})}{Q_{tot,n}} \tag{6.1}$$

where $Q_{tot,n}$ is the total heat loss from normal triple glazed window and $Q_{tot,a}$ is from the air flow window.

Figure 6.3 shows that the super version air flow window can achieve about 8% reduction of the total heat loss, including ventilation loss, for ventilation rates of 2 - 4 l/s per meter width of window. The reduction of total heat loss decrease for high ventilation flows because the ventilation heat loss becomes dominant. The standard version only reduces the total heat loss with 2-3 % for flows over 4 l/s.

6.1 Thermal Performance with Solar Irradiation.

The effect of solar irradiation is evaluated at reference winter conditions including solar irradiation of respectively 100, 300 and 500 $[W/m^2]$. In figure 6.4 are plotted the g-values as a function of the flow rate. The ventilation rate does not effect the g-value of normal windows. But the g-value for air flow windows increases with increased ventilation rate, because a larger portion of the radiation absorbed in the panes is utilized.

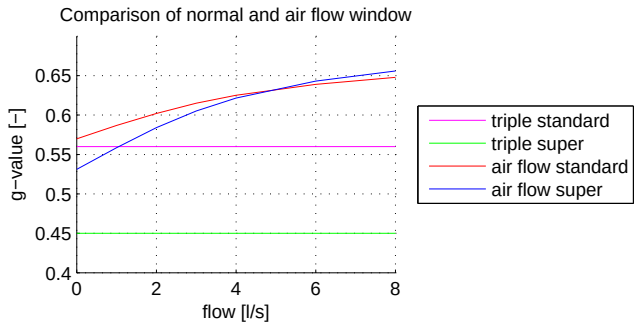

FIGURE 6.4: *Comparison of g-value for different ventilation flows.*

The g-value for normal windows depends mainly on the coatings and the absorption of the panes. The normal 'super' window has the lowest g-value because the low-emissivity coatings used are optimized for extremely low emissivity in favour of low reflectance. Low-emissivity coatings generally increase the reflectance, which lowers the g-values.

Figure 6.4 shows that the g-values of the air flow windows increase with ventilation flow and reach a g-value of about 0.65, or about 20 percentage points more than the super version of normal triple glazed window.

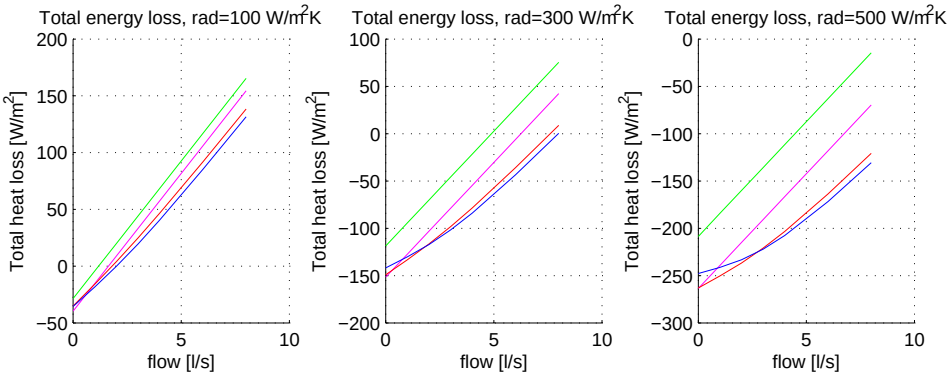

FIGURE 6.5: *Comparison of total heat loss with solar irradiation.*

The increase of the g-values with increased ventilation is also reflected in the total heat loss presented in figure 6.4. A negative total heat loss is actually a energy surplus. For ventilation rates of more than 2 $l/s$the air flow windows have the smallest total heat losses. The effect of utilizing the absorbed heat can also been seen in that while the 'super' air flow window has a lower direct solar transmittance than the standard, because of the hard low-emissivity coating, the g-value increase faster and ultimately to a higher level. For ventilation rates of more than 2-3 l/s has the 'super' air flow window the lowest total heat loss. But the difference between the standard and super version is quite small.

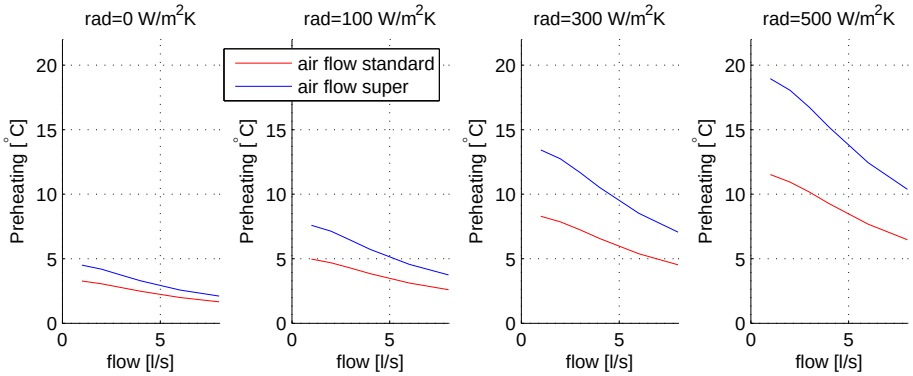

FIGURE 6.6: *Preheating of ventilation air as function of ventilation rate.*

The preheating of the ventilation air with and without solar irradiation is plotted in figure 6.6. For no solar irradiation the ventilation air is preheated

between 2 and 4 °C, decreasing with the ventilation rate. With solar irradiation of 500 W/m^2, the ventilation air is heated between 7 and 18 °C. The higher the ventilation rate the lower the preheating, because the air is less time in the cavity and therefore has less time to be heated. The 'super' version of the air flow windows preheats the ventilation air roughly 50 % more than the standard version.

6.2 Example of Heating Season Performance

An example of the heating season performances of air flow windows are evaluated by the BE06 programme[1]. The air flow windows are compared to normal windows both with exhaust ventilation and with heat recovery. The comparison is made for the heating season, here defined as from the beginning of October to the end of April because BE06 only calculates in full months.

The case is a 60 m^2 apartment, with a window area 25% of the flor area. The minimum mandatory exhaust ventilation is 35 l/s. For a ceiling height of 2.5 m, this gives an airchange of 0.84 times per hour.

property	value	unit
floor area	60	m^2
window area	15	m^2
ventilation	35	l/S
	0.84	h^{-1}
infiltration	18	l/s
	0.43	h^{-1}

TABLE 6.4: *Properties of apartment for evaluation of performance in heating season.*

Air flow windows have significant advantages when facing south because to the high g-values. To take into account that windows can not be expected to only face south, the windows are evenly distributed between facing north, south, east and west. The height of the windows is assumed to be 1.3 m. This results in an air flow rate of 3 l/s per meter width of windows, not considering the area of the frame. The normal windows are the triple glazed standard and super version presented on page 68. The configurations of the air flow windows are the same, but because of the increased height the thermal characteristics are different. the The thermal characteristics are presented in table 6.5 on the next page. Only the vision areas of the windows are considered.

[1] BE06 is the energy assessment program prescribed by the Danish building regulation code [2].

Cases with both exhaust ventilation and balanced ventilation with heat recovery, are included for normal windows. For the case with ventilation heat recovery, the temperature efficiency of the heat recovery is set to 0.85. But for balanced ventilation it is mandatory, according to the Danish building regulation code [2], to include an infiltration of $0.3\ l/s$ per square meter floor area[2]. The infiltration constitutes an airchange of roughly 0.5 times per hour. This of course greatly reduces the effect of the heat recovery.

type		normal windows		air flow windows	
quality		standard	super	standard	super
U-value	$[W/m^2K]$	0.82	0.72	0.75	0.47
g-value	[-]	0.56	0.45	0.78	0.77

TABLE 6.5: *Thermal performance characteristics of normal windows and air flow window with a height of 1.3 m and a air flow of 3 l/s.*

The energy balance for situations with exhaust and balanced ventilation are shown in table 6.6 on the facing page. The heat losses are shown as heat loss per square meter floor area. All the windows have an energy surplus, excluding the ventilation loss. The largest total heat losses are observed for normal windows with exhaust ventilation. The standard and super version differs only a little and have a total heat loss of respectively 952 and 913 kWh/m^2. The air flow windows perform considerably better with a total heat loss of respectively 748 and 660 kWh/m^2 for the standard and super version. The super version of the air flow windows reduces the total heat loss with roughly 30% compared to the normal windows.

For normal windows coupled with balanced ventilation with heat recovery it looks a bit different. The ventilation loss is reduced, but only about 30%, because the infiltration increases for balanced ventilation, and there is no heat recovery on the infiltration part. The total heat loss is 615 and 583 kWh/m^2 respectively for standard and super version of windows.

The minimum total heat loss is achieved with normal windows and balanced heat recovery ventilation. But the reduction is not very large compared to the air flow windows.

[2]If the buildings air-tightness has been measured, it is possible calculate the infiltration specific and lower infiltration rates can be used.

type	quality	Window loss $[kWh/m^2]$	Vent. loss $[kWh/m^2]$	Total loss $[kWh/m^2]$
Normal (exhaust)	standard	-55	1007	952
	super	-93	1007	913
Air flow	standard	-258	1007	748
	super	-347	1007	660
Normal (balanced)	standard	-55	670	615
	super	-93	670	583

TABLE 6.6: *Comparison of the heat loss per square meter floor area from the windows, including ventilation heat loss.*

6.3 Brief Reflections on Performance in Summer Conditions

This project has focus on the thermal performance of air flow windows in the heating season. How the windows perform in summer situations is of cause important. The large cavity invites to integrating solar shading. But it is given, that as long as the fresh air flows through the cavity, the solar energy transmittance will not be affected significantly. The solar energy trapped in the cavity by an integrated solar shading, will just cause extra preheating of the ventilation air.

If solar shading is integrated in the cavity, it is necessary that the ventilation air can bypass the cavity and be drawn in directly. PCvinduer [10] solve this problem by installing a temperature controlled valve that causes the heated air in the cavity to be returned to the outside and the fresh air intake to enter directly without preheating. Natural buoyancy will vent the cavity if it just is open to the environment in both top and bottom.

With an efficient control of valves and solar shading, air flow windows can potentially achieve very flexible combination of glare control, solar energy control and low U-values.

6.4 Conclusion

Two different configurations of air flow windows have been evaluated. On with and one without a low-emissivity hard coating on one surface in the cavity. Comparisons between normal windows and air flow windows have shown that air flow windows have some significant advantages in situations

with exhaust ventilation.

Both the U-value and the g-value depend on the flow rate. The effective U-value drops rapidly with increased ventilation rate. Already at 2 l/s is the effective U-value of the hard-coated version $U_{eff} \approx 0.5\ W/m^2K$. For flows larger than 6 l/s is $U_{eff} < 0.2\ W/m^2K$.

The solar energy transmittance in return increases with increased ventilation flow. A larger portion of the solar energy absorbed in the panes is utilized, because the ventilation air effectively cool down the panes while being preheated. Because of the lower temperature of the panes less heat are lost to the environment than for normal windows.

The performance of air flow windows can be greatly increased with a low-emissivity coating on one side of the cavity, even though only hard coatings are feasible. The direct solar transmittance is lowered by the coating, but this is compensated by increased preheating of the ventilation air. For flows larger than 2 l/s the hard coated version of the air flow window has both the lowest effective U-value and the highest solar energy transmittance, g-value.

Air flow windows can outperform even the best normal window with regard to solar energy transmittance and heat loss. But the air flow window is not a miracle cure. The increased performance can not outweigh the resulting ventilation loss. The apartment example for the heating season show, that the air flow windows can reduce the total heat loss from windows and exhaust ventilation by almost 30%. But it is still better to have balanced ventilation with heat recovery, even whit increased infiltration.

Chapter 7

Conclusion

This report demonstrates that the air flow window principle can be used to lower the heating demands in buildings ventilated by exhaust ventilation. Focus is on a 1+2 configuration of the ventilation window, with the air flowing upwards in the cavity. By drawing the ventilation air through the cavity between the panes before it enters the room, it is possible to reduce the transmissive heat loss through the window, and at the same time preheat the ventilation air.

The main aim of this project is to establish a method for predicting the thermal performance of air flow windows. It is demonstrated that the existing ISO standard method is inadequate to predict the convective heat fluxes in the ventilated cavity. Therefore an alternative transient finite difference method is proposed and verified against CFD simulations. The transient method proves to be significant improvement of the ISO standard.

Based on the ISO standard a program (WinVent) is developed to calculate the thermal performance of windows. Using the proposed transient method, WinVent is used to calculate the performance of air flow windows. Two different configurations of air flow windows have been evaluated. One with and one without low-emissivity hard coating on one surface in the cavity. Comparisons between normal windows and air flow windows have shown that air flow windows have some significant advantages in situations with exhaust ventilation.

7.1 CFD Simulations

Because of the short time frame, and the need to conduct a large range of parameter studies, CFD modelling was chosen as the tool of investigation. The CFD model is verified by grid dependency analysis and by verifying the

results of the well known and extensively researched case of natural convection in a closed vertical cavity. The ReNormalisation Group (RNG) turbulence model is found to produce the overall best results.

CFD simulation is used to conduct parameter studies of the influence of flow rate, solar irradiation, cavity depth and cavity height.

7.1.1 Prediction of Heat Fluxes in Ventilated Cavity

The ISO standard method is found to be inadequate to predict the convective heat fluxes. The fundamental assumption behind the method is that the cavity air temperature can be represented by the volume average temperature. But it is shown that the volume average can not adequately represent the asymmetrical temperature profiles found by the CFD simulations. It is therefore necessary to abandon the average air temperature as representation of the cavity air temperature in order to improve the method. It is possible, that by introducing an arbitrary air temperature dependent on only one of the surfaces heat transfer coefficients, predictions by the method can be improved. But the very asymmetrical temperature profiles found in the cavity makes it unlikely that the air temperature can be adequately represented by one temperature node.

Analyzing temperature profiles of the air in the cavity it was found the temperature developments up through the cavity show similarities with one-dimensional transient temperature developments, as found in a wall suddenly exposed to asymmetrical temperatures on opposite sides. Based on this a transient one-dimensional conduction method is developed. The time dependency is linking to the height of the cavity by use of the average velocity of the air.

Based on simple assumptions of conductivity the transient method is found to produce remarkably better results than the original ISO standard method. But the assumptions behind the transient method are not valid for flows highly dominated by natural buoyancy, which results in a overestimation of the heat loss for low ventilation rates. Low ventilation rates being in the investigated cases, $\varphi < 2 \quad [l/s]$ per meter width of window. The transient method is not able to predict the improved performance of increasing the depth of the cavity either. So even though the proposed transient method is a significant improvement compared to the ISO standard method, the transient method has a tendency to underestimate the thermal performance for cases with low ventilation rates or increased cavity depth.

Implementing the transient method in WinVent has shown that changing the method for the ventilated cavity from the ISO standard to the transient method has a large impact on the effective U-value (9 to 33 % reduction) and a on the preheating of the ventilation air (20 to 40 % increase). The impact on

the g-value is more modest with an increase of 2 to 3 %.

7.2 Thermal Performance of Air Flow Windows

Two different configurations of air flow windows are evaluated and compared to normal triple glazed windows in situations with exhaust ventilation.

The performance of air flow windows can be greatly increased with a low-emissivity coating on one side of the cavity, even though only hard coatings are feasible. The direct solar transmittance is lowered by the coating, but this is compensated by increased preheating of the ventilation air. For flows larger than 2 l/s has the hard coated version of the air flow window both the lowest effective U-value and the highest solar energy transmittance, g-value.

Air flow windows have the great advantage over normal windows that they can achieve both an extremely low heat loss and a high solar energy transmittance at the same time. The effective heat loss coefficient, U_{eff} and the total solar transmittance, g-value depend on the flow rate. The effective U-value drops rapidly with increased ventilation rate. The hard coated version of the air flow winds achieves an effective U-value of $U_{eff} \approx 0.5\ W/m^2K$ already at 2 l/s. For flows larger than 6 l/s the effective U-value drops to the very low $U_{eff} < 0.2\ W/m^2K$.

The solar energy transmittance in return increases with increased ventilation flow. The ventilation air cool down the panes effectively – especially the outer pane. Because of the lower temperature of the outside pane less heat is lost to the outside environment, and a larger portion of the solar irradiation absorbed in the panes can be utilized. Therefore air flow windows achieve much larger g-values than normal triple pane windows.

Air flow windows can outperform even the best normal window with regard to solar energy transmittance and heat loss. But the air flow window is not a miracle cure. The increased performance can not outweigh the resulting ventilation loss. An example of an apartment shows, that the air flow windows can reduce the total heat loss from windows and exhaust ventilation by almost 30%. But the lowest heat loss is achieved by normal windows and balanced ventilation with heat recovery.

Many buildings are constructed with only exhaust or natural ventilation. Changing the windows to air flow windows can be a relatively cheap an easy energy renovation. As opposed to installing balanced ventilation with heat recovery, exchanging the windows and perhaps installing exhaust ventilation doesn't demand large spaces for ducts and ventilation equipment. This project provides a firm basis for evaluation of the thermal performance of air flow windows in the heating season. A basis that can be used by window producers,

building energy consultants or other interested parties to promote air flow windows as tool for lowering heating demands.

7.3 Further Work

While contributing with an important basis for advancing the knowledge and use of air flow windows, this project only lays out a promising path to follow. Many issues still needs to be understood better for the potential of air flow windows to be fully utilized. Not to mention the task of optimizing the design – including design of frame and valves. This chapter concerns ideas to projects which could be made in continuation of the present project.

The transient method developed and proposed in this project is based on very simple assumptions of the thermal conductivity and heat capacity. It is therefore likely that there is room for improvement. If the method is to be made valid for flows highly dominated by natural buoyancy it is properly necessary to extent the method to a 2-dimensional finite difference or in some other way account for the swirling flow.

One of the proposed, but not investigated, solutions to improve the performance in summer situations is to incorporate solar shading in the cavity. Whether roller screen or blinds, integrating a solar shading will effect the air flow pattern and convective heat flows. In order to evaluate the air flow windows in summer situations it is necessary to be able to predict to solar energy transmittance when solar shadings are integrated. In summer situations the air in the cavity will most likely be returned to the outside and the ventilation air drawn in directly.

Many low-energy houses have implemented a heat pump in the ventilation system to produce domestic hot water. But the passive heat recovery and the heat pump can not be active at same time, which reduces the effectiveness of the system. It could be interesting to investigation the performance of a system combining air flow windows and active ventilation heat recovery by placing the heat pump collector in the exhaust ventilation. Drawing heat out of the exhaust ventilation is much more efficient than placing the heat collector in the outside environment because the temperature differential is much smaller. Such a system might provide enough energy for both domestic hot water and the heating system.

But any further work on air flow windows could greatly benefit from experimental testing. Both in order to validate the simulations and to investigate the influence of valve and frame design.

Bibliography

[1] Bygge og Boligstyrelsen. *Bygningsreglement af 1977 (inkl. tillæg 1-15)*. 1977.

[2] Erhvervs og Boligstyrelsen. *Bygningsreglement for erhvervs- og etagebyggeri (inkl. tillæg 1-15)*. 2007.

[3] Henrik Tommerup. Energibesparelse for "ventilationsvindue". Sagsrapport SR-05-01, BYG•DTU, 2005.

[4] Dirk Saelens. *Energy performance assesments of single storey multiple-skin facades*. PhD thesis, Katholieke universiteit Leuven, 2002.

[5] Tapio Korkala. Air intake arrangements of the supply air window from the view of comfort and ventilation efficiency. *Swedish Council for Building Research*, pages 466–472, 1984.

[6] J. R. McDaniel. Uncharted assets of the air flow window system. *Swedish Council for building Research*, pages 144–149, 1987.

[7] P. H. Baker and M. McEvoy. Test cell analysis of the use of a supply air window as a passive solar component. *Solar Energy*, 69(2):113–130, 2000.

[8] R.G.and McEvoy M. E. Southall. investigations into the functioning of a supply air window in relation to solar energy as determined by experiment and simulation. *Solar Energy*, 80:512–523, 2006.

[9] Hansengroup promotes a sound reducing "3g-window" that incorporates aspects of air flow windows. `http://www.servicehansen.com/hansengroup/product3gwindow.php?lang=da&cp=`.

[10] Pc vinduer promotes a patented air flow window. `http://www.pcvinduer.dk/p215.asp`.

[11] ISO 15099. Thermal performance of windows, doors and shading devices - detailed calculations. Technical report, 2003.

[12] International building physics toolbox. The Toolbox is a library of Simulink blocks specially designed for HAM system analyses in Building Physics. The project is initiated by two research teams: Building Physics Department from Chalmers University of Technology, Sweden, and Department of Civil Engineering from Technical University of Denmark. For more information information on Building Physics Toolbox `www.ibpt.org`.

[13] Buildingcalc. The Matlab program BuildingCalc has been developed to evaluate the demands for heating and cooling and the indoor temperature on an hourly basis. The program uses a very simplified mathematical model of the building. Heating, cooling, solar shading, variable air volume ventilation and venting can be applied to control the indoor temperature. It is developed at the Department of Civil Engineering from Technical University of Denmark. For more information on BuildingCalc `www.dtu.dk/centre/BFI/Om%20BFI/Medarbejdere/trn.aspx`.

[14] Bsim. BSim is an integrated PC tool for analysing buildings and installations. BSim includes tools for simulating and calculating e.g. thermal indoor climate, energy consumption, daylight conditions, synchronous simulation of moisture and energy transport in constructions and spaces and calculation of natural ventilation. BSim is developed by the Danish Building Research Institute For more information on BSim `www.en.sbi.dk/publications/programs_models/bsim`,.

[15] Iesve. The IES ¡Virtual Environment¿ is a software system of integrated building performance analysis tools. IESVE includes tools for simulating and calculating e.g. thermal indoor climate, energy consumption, daylight conditions by ray tracing and calculation of multizone natural ventilation. For more information on IESVE `www.iesve.com`.

[16] *FLUENT User Manual*.

[17] S.H. Yin, T.Y. Wung, and K. Chen. Natural concevtion in an air layer enclosed within rectangular cavities. *International Journal of Heat and Mass Transfer*, 21:307–315, 1978.

[18] Sylvie Lorente. Heat losses through building walls with closed, open and deformable cavities. *International Journal of Energy Research*, (20):611–632, 2002.

[19] Guohui Gan. Thermal transmittance of multiple glazing: computational fluid dynamics predection. *Applied thermal Engineering*, 21:1583–1592, 2001.

[20] Bérengère Lartigue, Sylvie Lorente, and Bernard Bourret. Multicellular natural convection in high aspect ration cavity: experimental and numerical results. *International journal of Heat and Mass Transfer*, 34:3157–3170, 2000.

[21] Bhaskar Adusumalli. Modeling natural convection in glazin cavity and predecting transition limits for multicellular flow from simulations on fluent. Technical report, CEERE - Center for Energy Efficiency and Renewable energy, University of Massachusetts, Department of Mechanical and Industrial Engineering, August 2003.

[22] Frank P. Incropera and David P. DeWitt. *Indtroduction To Heat Transfer*. John Wiley & Sons, 2002.

[23] Anthony F. Mills. *Heat Transfer*.

[24] Yougesh Jaluria and Kenneth E. Torrance. *Computational Heat Transfer*. Series in Computational Methods in Mechanics and Thermal Science. Taylor & Francis, New York, second edition edition, 2003.

List of Figures

List of Tables

Appendix A

Velocity and temperature profiles

A.1 Variation of flow

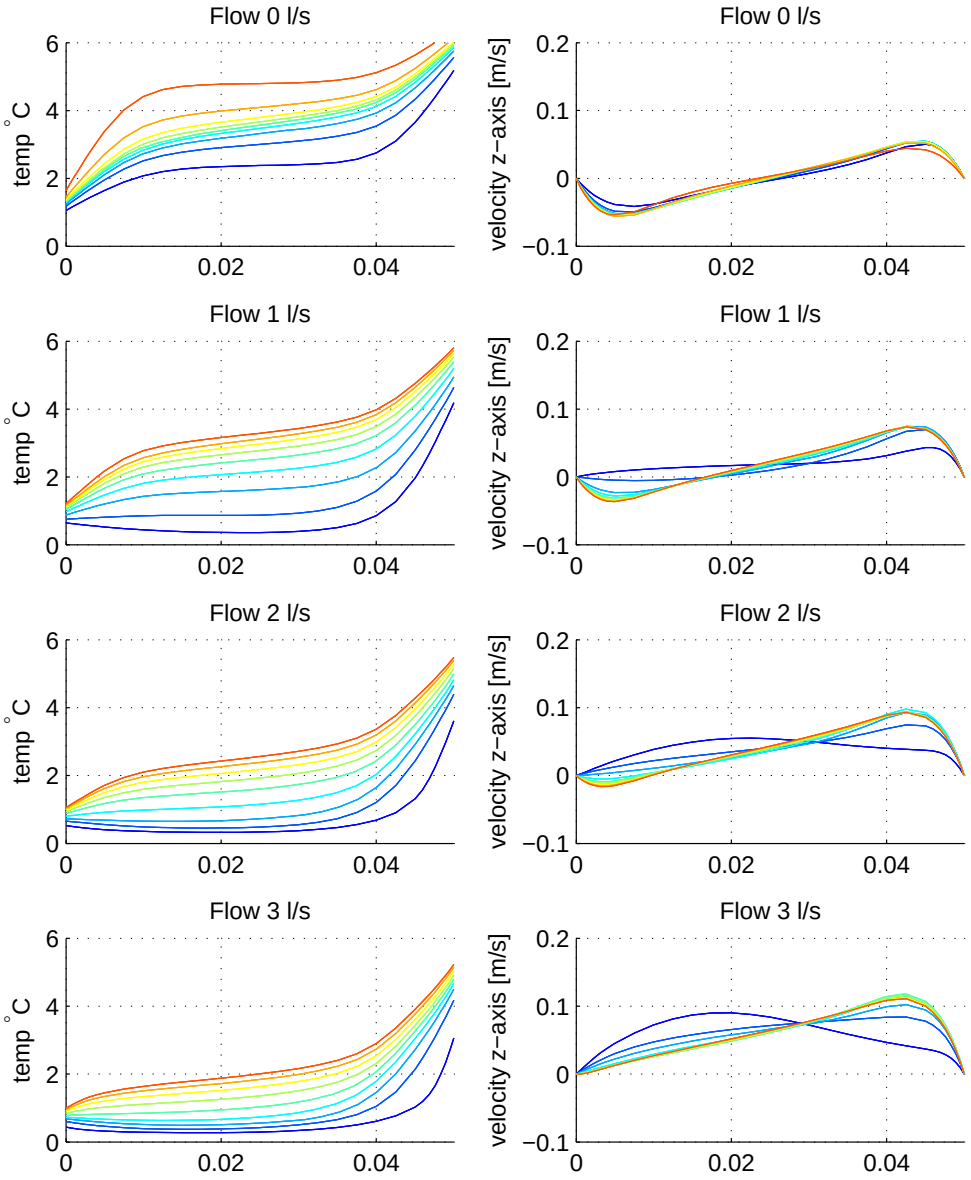

FIGURE A.1: *Flow profiles for 0 to 4 l/s flow – no solar irradiation.*

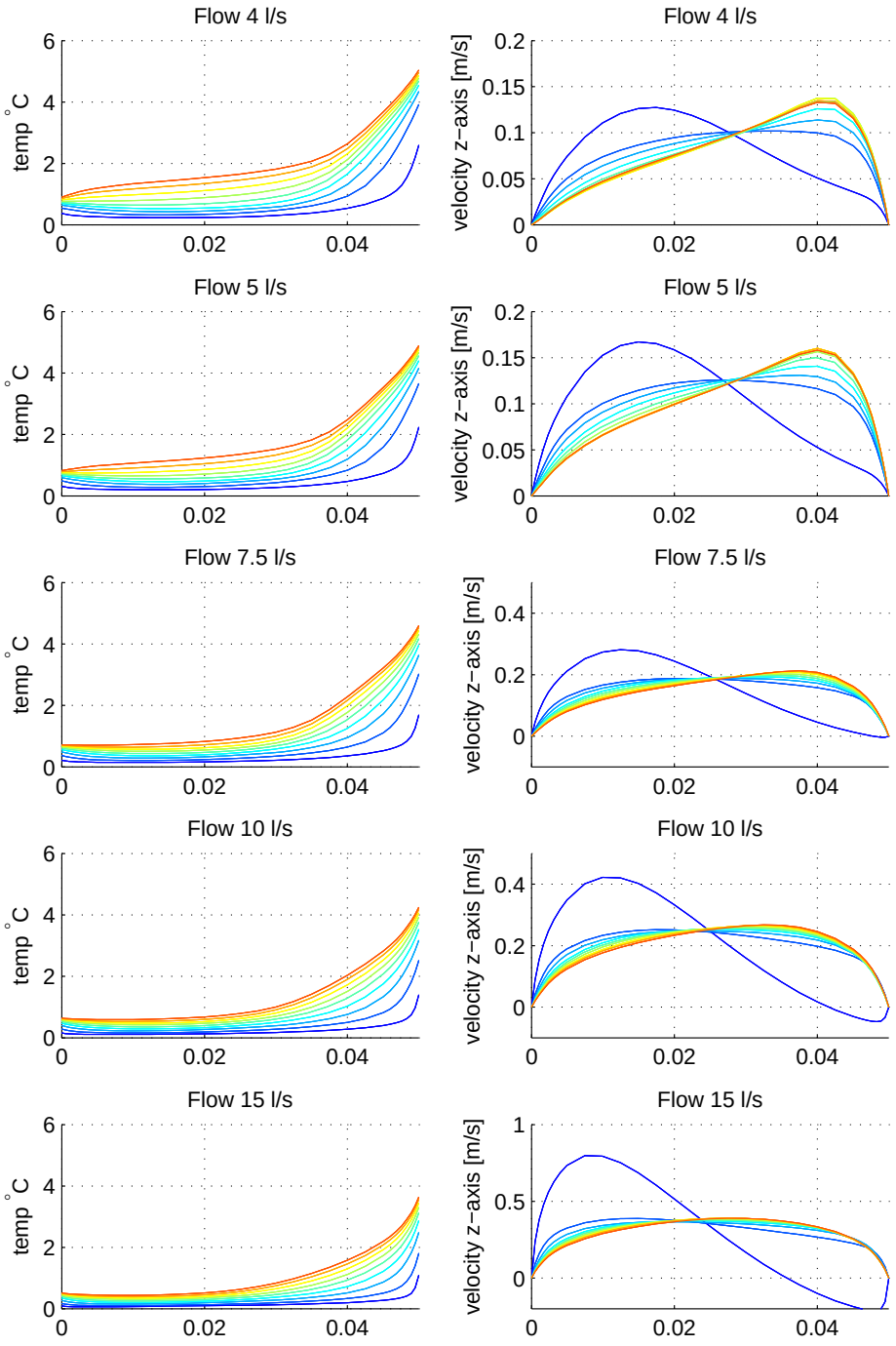

FIGURE A.2: *Flow profiles for 5 to 15 l/s flow – no solar irradiation.*

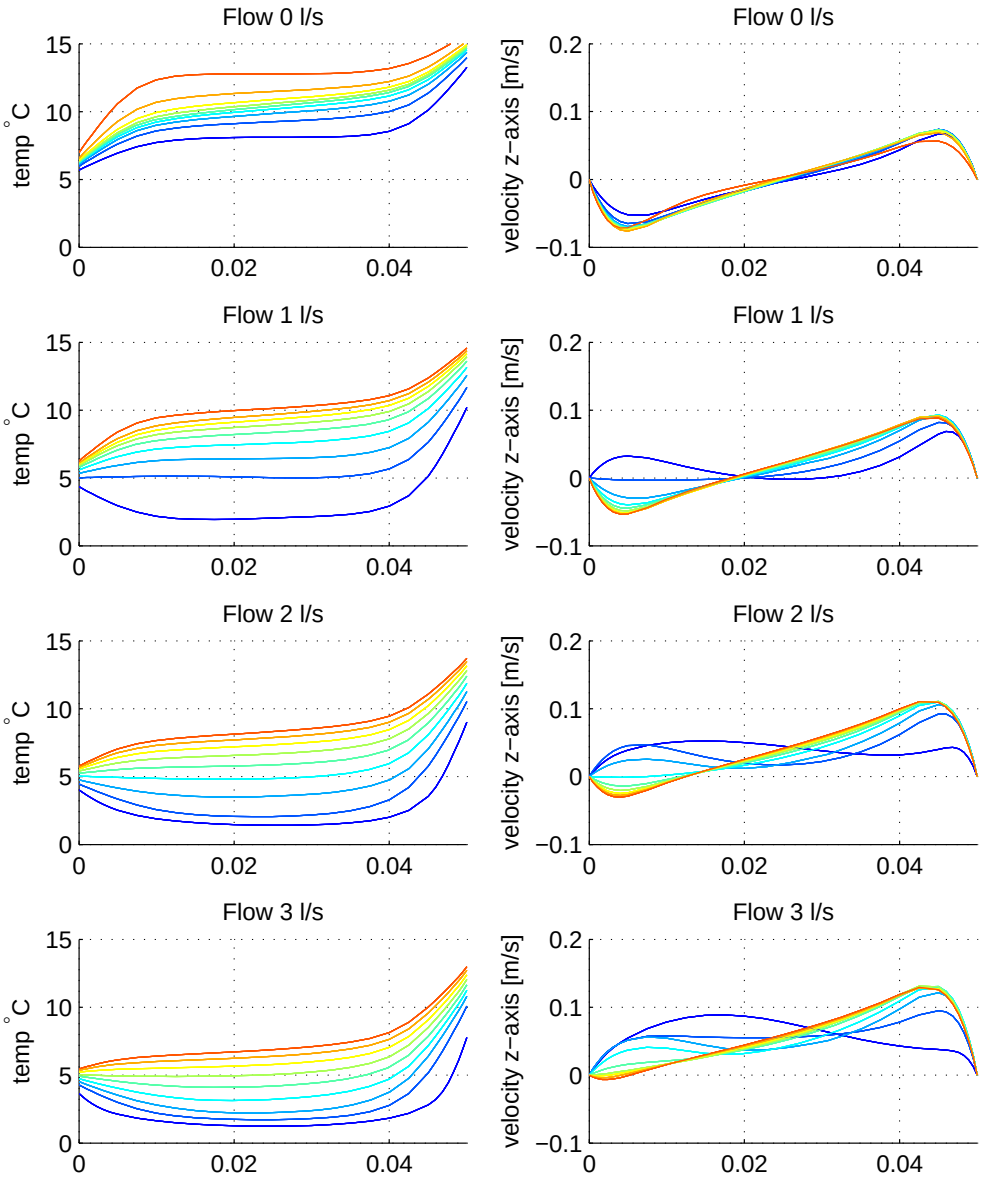

FIGURE A.3: *Flow profiles for 0 to 4 l/s flow – 500 W/m^2 solar irradiation..*

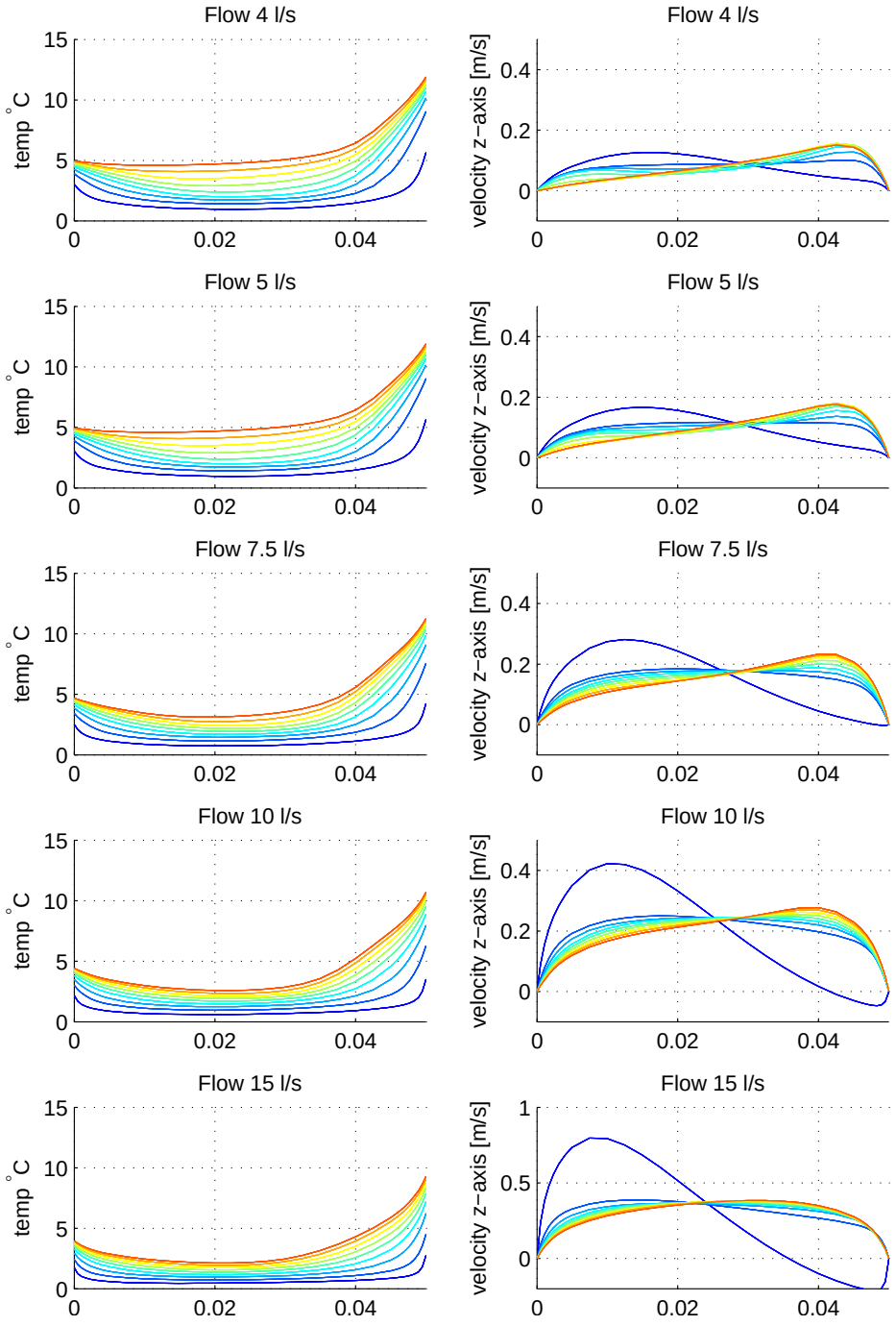

FIGURE A.4: *Flow profiles for 5 to 15 l/s flow – 500 W/m^2 solar irradiation..*

A.2 Variation of solar irradiation

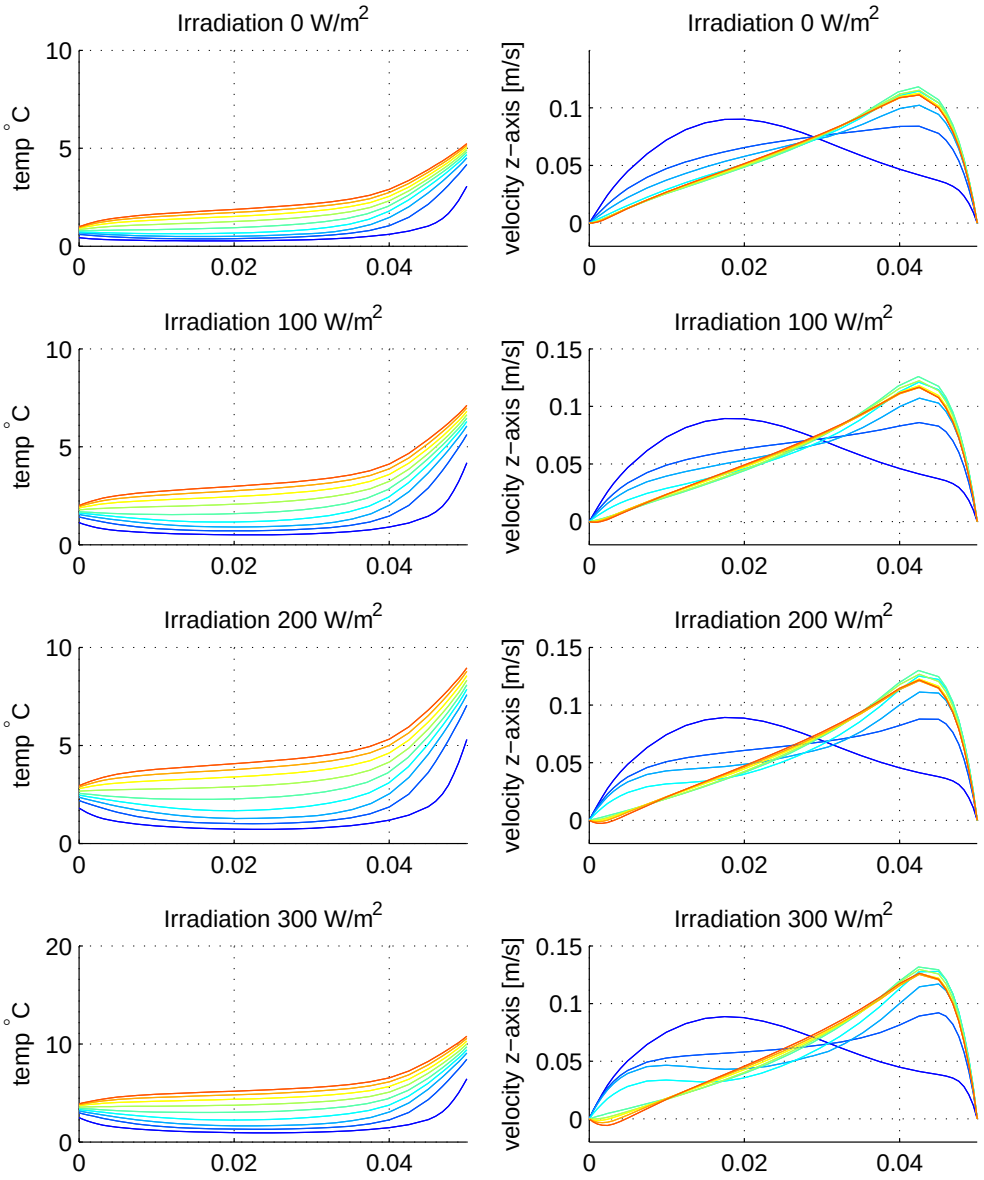

FIGURE A.5: *Flow profiles for 0 to 300 $W/m^2$2 irradiation – 3 l/s flow.*

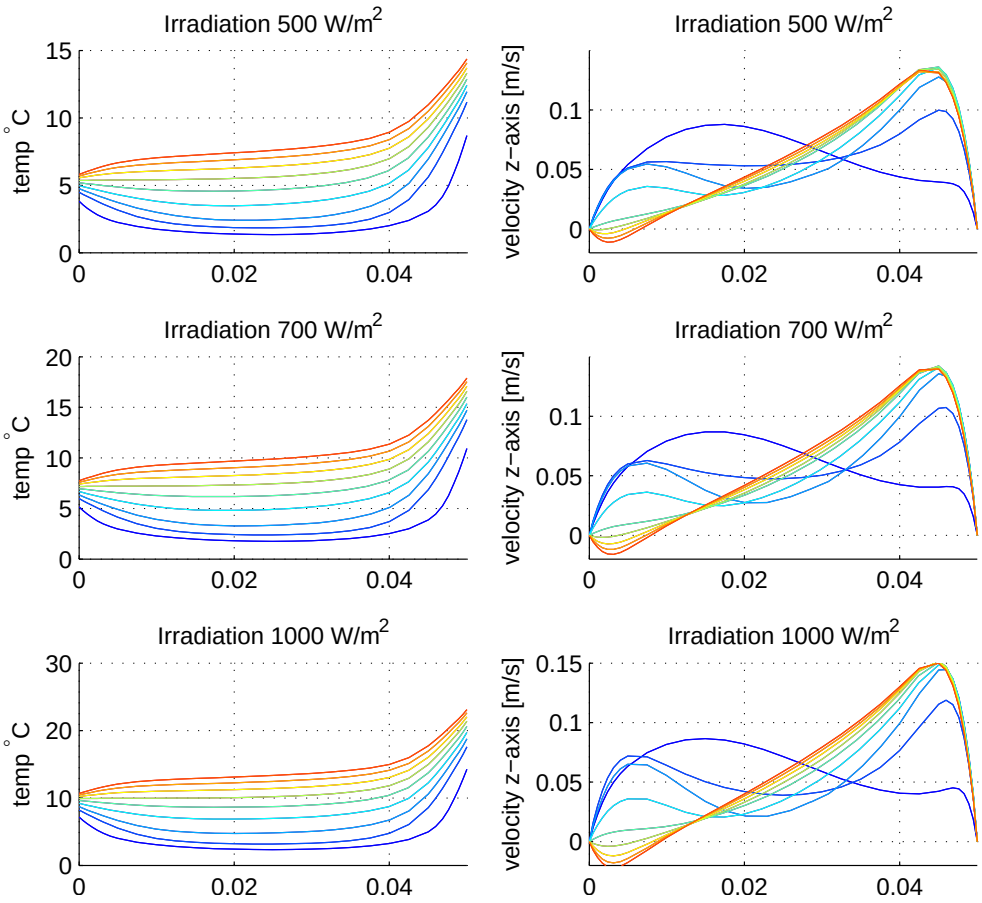

FIGURE A.6: *Flow profiles for 500 to 1000 $W/m^2$2 irradiation – 3 l/s flow.*

A.3 Variation of cavity depth

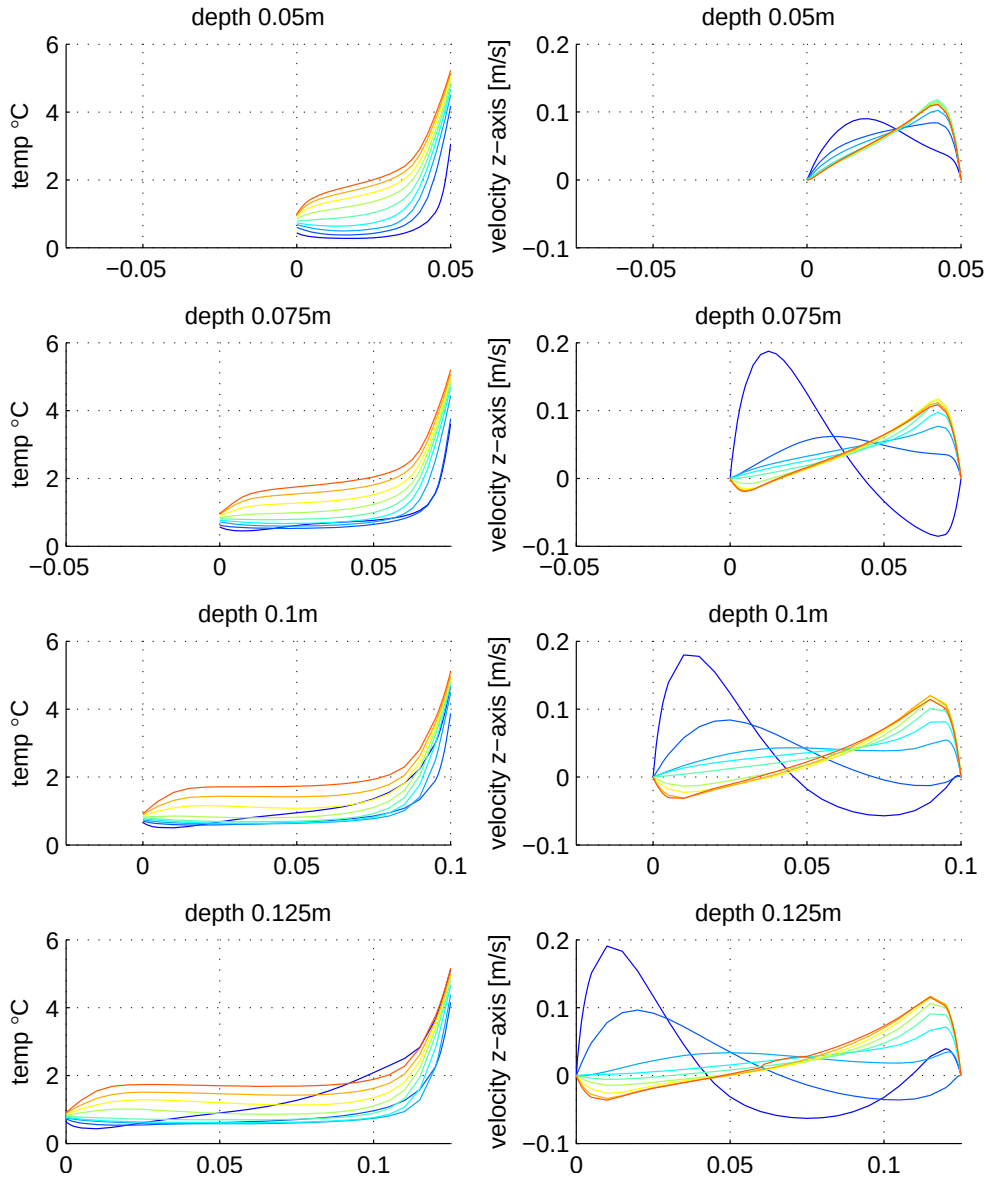

FIGURE A.7: *Flow profiles for 50 to 125 mm cavity depth – 3 l/s flow.*

A.4 Variation of cavity height

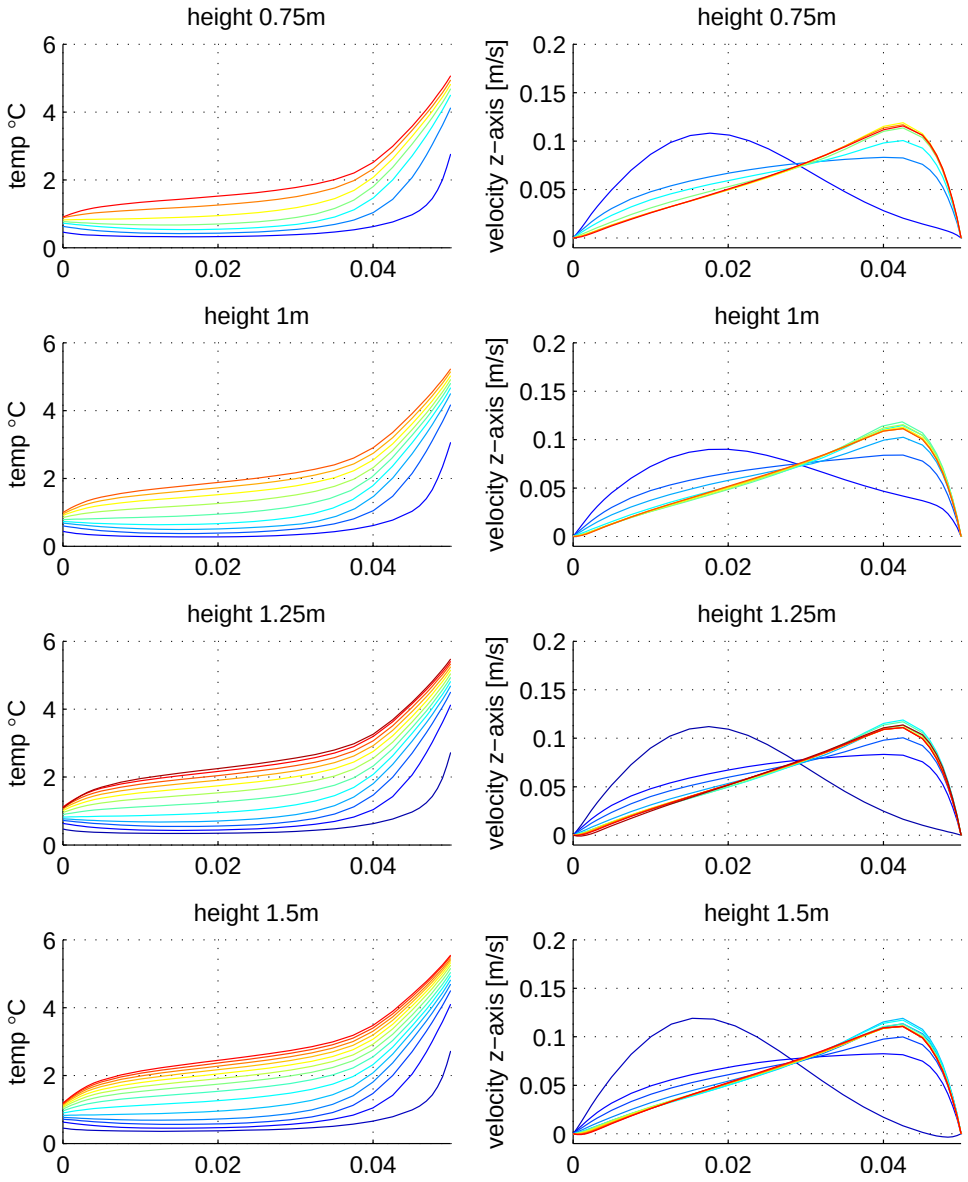

FIGURE A.8: *Flow profiles for 0.75 to 1.50 m cavity height – 3 l/s flow.*